TÉCNICO LISBOA

Continuous Manoyl Oxide production by a genetically modified strain of *C. reinhardtii*

Sara Soares Cidraes Vieira

Thesis to obtain the Master of Science Degree in

Energy Engineering and Management

Supervisors: Dr. Iago Dominguez Teles

Prof. Ana Paula Vieira Soares Pereira Dias

Examination Committee

Chairperson: Prof. Francisco Manuel da Silva Lemos

Supervisor: Prof. Ana Paula Vieira Soares Pereira Dias

Member of the Committee: Dr. Maria Teresa Ferreira Cesário Smolders

December 2019

Acknowledgements

My sincere thank you…

to Iago, for keeping me in solid ground every time I wanted to slip;
to Josué, for turning on the light when I was aiming in the dark;
to Ana Paula Dias and Mariusz Wądrzyk for boarding towards the unknown with me;
to Thomas Baier and Alexander Einhaus for all the patience and help with the GC-MS analysis;
to Maria Barbosa and Helena Luísa for making a wish come true;
to all the people I had the pleasure to work with at BPE, for all the support you gave me and all the lessons I take from you;
to all my friends at BPE, with who a daily frustrations exchange was always a learning moment, for all the good laughs at our coffee corner and perfect partnerships in the lab;
to all my friends in Wageningen, who welcomed me in the city of life sciences and turned it into a place I always wish to return – now I know why people stay there for so long;
to all my friends from this master programme: you made Poland my home, while making it your own – it was an honour to grow in your company and to see you grow in mine;
to all my friends and family in Lisbon, my charging station after each adventure, for being there for me even though I insist in running away;
and because the firsts come in last, to my parents, the ultimate supporters of anything I do in life.

Abstract

Genetically modified strains of *Chlamydomonas reinhardtii*, tailored for the production and excretion of the terpenoids 13R(+)-Manoyl Oxide and 9-hydroxy-Manoyl Oxide, were used in the current work. Both compounds are precursors of forskolin, a potential pharmacy drug. The terpenoids were then extracted by keeping the culture in contact with a dodecane overlayer. Up to 6.7 mg of Manoyl Oxide and 1.8 mg of 9-hydroxy-Manoyl Oxide per gram of dry biomass per day were obtained from cultures growing in batch in Erlenmeyer flasks.

The aim of this thesis was to design and test a continuous and scaled up set up for the simultaneous production and extraction of these products. The set up consisted of circulating the microalgae between a flat panel photobioreactor and an extraction vessel, where they would contact the extraction solvent. In 400 mL reactors, 1.8 mg of Manoyl Oxide and 0.40 mg of 9-hydroxy-Manoyl Oxide per gram of dry biomass per day were extracted. Up to 0.76 mg of Manoyl Oxide and 0.17 mg of 9-hydroxy-Manoyl Oxide per gram of dry biomass per day were reached in 1.8 L reactors, where different biomass concentrations and light intensities were tested. A cell death rate between 7 and 9% was observed for the overall process.

The second objective was to further understand the production, excretion and extraction dynamics of the system, to which the remaining terpenoids content inside the cells and in the aqueous phase was assessed. A mass transfer coefficient of $(4.9\pm1.0)10^{-5}$ day^{-1} and $(1.1\pm0.4)10^{-5}$ day^{-1} was calculated for Manoyl Oxide in the Erlenmeyer flasks and in the 1.8 L reactors, respectively. In the Erlenmeyers, the production rates were $(6.6\pm0.1)10^{-3}$ $gL^{-1}day^{-1}$ for Manoyl Oxide and $(1.7\pm0.1)10^{-3}$ $gL^{-1}day^{-1}$ for 9-hydroxy-Manoyl Oxide, while $(1.2\pm0.3)10^{-3}$ $gL^{-1}day^{-1}$ and $(2.4\pm1.4)10^{-4}$ $gL^{-1}day^{-1}$ were obtained in the 1.8 L reactors for Manoyl Oxide and 9-hydroxy-Manoyl Oxide, respectively.

Keywords: *Chlamydomonas reinhardtii, Terpenoids, Manoyl Oxide, Drug precursor, Continuous extraction, Scale up*

Resumo

Neste trabalho usaram-se estirpes de *Chlamydomonas reinhardtii* geneticamente modificadas para a produção e excreção dos terpenóides 13R(+)-Óxido de Manoil e 9-hidroxi-Óxido de Manoil. Ambos são precursores de forskolin, um composto com potencial enquanto fármaco. A extração dos terpenóides foi conseguida mantendo-se a cultura em contacto com uma camada de dodecano, obtendo-se até 6,7 mg de Óxido de Manoil e 1,8 mg de 9-hidroxi-Óxido de Manoil por grama de biomassa seca e por dia para culturas a crescer em *Erlenmeyers* em modo *batch*.

O objetivo desta tese era projetar e testar uma montagem para a produção e extração contínua e *scaled-up* destes produtos. A montagem permitia a circulação das microalgas entre um fotobioreactor de painel plano e um recipiente onde entravam em contacto com o solvente de extração. Nos reatores de 400 mL conseguiu-se extrair 1,8 mg de Óxido de Manoil e 0,40 mg de 9-hidroxi-Óxido de Manoil por grama de biomassa seca e por dia. Nos reatores de 1,8 L, onde se testaram diferentes intensidades de luz e concentrações de biomassas, atingiu-se até 0,76 mg de Óxido de Manoil e 0,17 mg de 9-hidroxi-Óxido de Manoil por grama de biomassa seca e por dia. Observou-se uma taxa de morte celular de 7 a 9% em todo o sistema.

O segundo objetivo era avaliar a dinâmica da produção, excreção e da extração do sistema, para o qual os restantes terpenóides, que permaneceram dentro das células e na fase aquosa, foram também analisados. Foi calculado um coeficiente de transferência de massa para o Óxido de Manoil de $(4,9\pm1,0)10^{-5}$ dia^{-1} e $(1,1\pm0,4)10^{-5}$ dia^{-1} nos frascos *Erlenmeyer* e nos reatores de 1,8 L, respetivamente. As taxas de produção nos Erlenmeyers foram de $(6,6\pm0,1)10^{-3}$ $gL^{-1}dia^{-1}$ para o Óxido de Manoil e $(1,7\pm0,1)10^{-3}$ $gL^{-1}dia^{1}$ para o 9-hidroxi-Óxido de Manoil, enquanto nos reatores de 1,8 L se obtiveram $(1,2\pm0,3)10^{-3}$ $gL^{-1}dia^{-1}$ e $(2,4\pm1,4)10^{-4}$ $gL^{-1}dia^{-1}$ respetivamente para o Óxido de Manoil e 9-hidroxi-Óxido de Manoil.

Palavras-chave: *Chlamydomonas reinhardtii, Terpenóides, Óxido de Manoil, Precursor de fármaco, Extração contínua, Scale up*

Index

Index of figures

Index of tables

List of abbreviations and symbols

MO	13R(+)-Manoyl Oxide
9OH-MO	9-hydroxy-Manoyl Oxide
TAP Medium	Tris-Acetate-Phosphate Medium
TP Medium	Tris-Phosphate Medium
T2P 2N Medium	Tris-Phosphate Medium with twice the phosphate and nitrogen concentration
MP Medium	Mops-Phosphate Medium
OD	Optical Density measured at 750 nm wavelength
GC-FID	Gas Chromatography with Flame Ionization Detector
GC-MS	Gas Chromatography with Mass Spectrometry

x	g/L	Biomass concentration
μ	day^{-1}	Specific growth rate
Q	L/day	Flow of growth media
V_R	L	Volume of the aqueous phase in the system
V_{DD}	L	Volume of the dodecane phase in the system
m_{MO}^{X}	g/g	Manoyl Oxide concentration in the pellet
m_{MO}^{DD}	g/L	Manoyl Oxide concentration in the dodecane phase
m_{MO}^{AQ}	g/L	Manoyl Oxide concentration in the aqueous phase
r_{MO}	$gL^{-1}day^{-1}$	Manoyl Oxide production rate
r_{EX}	$gL^{-1}day^{-1}$	Manoyl Oxide excretion rate
k_T	$m^{-2}Lday^{-1}$	Mass transfer coefficient
a	m^2L^{-1}	Concentration of exchange area
K_4	g/g	Equilibrium constant between the Manoyl Oxide concentration in both the aqueous and organic phases
r_X	$gL^{-1}day^{-1}$	Biomass production rate
X	$gL^{-1}day^{-1}$	Fraction of Manoyl Oxide productivity in the pellet
D	$gL^{-1}day^{-1}$	Fraction of Manoyl Oxide productivity in the dodecane
AQ	$gL^{-1}day^{-1}$	Fraction of Manoyl Oxide productivity in the aqueous phase

1. Introduction

Microalgae contain a variety of valuable components, from pigments to lipids, proteins and vitamins. Moreover, genetic engineering has turned this simple organism into a powerful biochemical synthesis platform, allowing the production of specific compounds with higher titres and selectivity than before (Khan *et al.* 2018). Additionally, microalgae can rely mostly on sun light and carbon dioxide, which can be captured from industry or atmosphere, and does not compete with arable land or potable water (Khan *et al.* 2018, Laurens 2017). Some species can even be grown on wastewater, assisting on its treatment and allowing nutrient recovery (Molazadeh *et al.* 2019). For these reasons, microalgae are believed to have an important role in building a sustainable future. One of the biggest challenges from using microalgae to obtain valuable products is their further extraction from the cell (Islam *et al.* 2017). It often requires the use of energy intensive processes or toxic organic solvents, which has generated interest in compounds that can be both synthesized and excreted by the cells and on the development of genetically modified strains to do so.

In this thesis, two genetically modified strains of *Chlamydomonas reinhardtii* were used, tailored for the production and excretion of the terpenoids 13R(+)-Manoyl Oxide and 9-hydroxy-Manoyl Oxide. Both compounds are precursors from forskolin, which has promising applications in the medical field (Khatun 2011). In order to stimulate the production and extract these terpenoids, the microalgae were kept in contact with a dodecane layer, to which they have a higher affinity for than for the aqueous phase. This was already being done successfully in Erlenmeyer flasks, where the microalgae were growing in batch while the produced Manoyl Oxide and its hydroxylated form were being extracted in situ *(Lauersen et al.* 2018).

The first goal from this thesis was to design and test a scaled up and continuous process for the production of terpenoids from this microalgae strain. This was achieved by creating a circulation system between the growth chamber from lab-scale reactors and an extraction vessel, where the microalgae would be in contact with the dodecane phase. The second objective was to further study and understand the production, excretion and extraction dynamics of the system, paving the way for further optimization and outdoor scale-ups. This work was developed within the MERIT project, which is aimed at designing microalgal strains for optimized diterpenoid production and respective extraction, along with the process' scale up (MERIT).

2. Theoretical Background

Microalgae are unicellular photosynthetic organisms, comprising a huge number of species arranged in different phyla, spread even amongst different kingdoms. The majority of microalgae are eukaryotic, with the exception of cyanobacteria which are prokaryotes (Borowitzka 2016). That being said, there is a wide range of conditions were microalgae can prosper, which brings flexibility to the use and study of microalgae.

2.1. Microalgae Cultivation

Microalgae can be cultivated both in open or closed system, either outdoor or indoor. As expected, controlling temperature and light intensity are limited actions in outdoor installations, which may lead to inconsistent growth rates, but these have considerably lower operating costs than indoors (Chisti 2007). Open systems consist mainly on open pounds or raceway pounds, given that the first has fell in disuse and substituted by more efficient alternatives. Raceway pounds consist on shallow ring-channel circuits where the water motion and mixture are promoted by a paddle wheel (Figure 1). They are the cheapest microalgae cultivation system and extremely cost-effective, despite the very low productivities derived from poor light penetration and huge risk of contaminations. They have no oxygen oversaturation issues but are vulnerable to the external conditions and evaporation. A way to avoid contaminations is to grow algae tolerant to extreme conditions, such as high alkalinity, high salinity or high nutrients environments. However, such technique only works with a limited number of strains, and despite some records of growing microalgae in mild conditions with no significant contaminations (Bahadar and Bilal Khan 2013), open systems are not an option when an axenic culture is needed.

Figure 1: Raceway pound at AlgaePARC (Wageningen, Netherlands).

Closed photobioreactors appeared as an answer to open system's disadvantages. They are characterised by higher biomass productivities and a more sterile environment, which not only protects the culture from the environment, but also the environment from the culture, allowing the use of organic

carbon-rich medium (Bahadar and Bilal Khan 2013), keeping high purity cultures, and the growth of foreign and genetically modified strains. There are several different photobioreactor designs, varying its configuration, orientation or material. One of the key parameters to take into consideration is the light penetration, directly connected to the surface area to volume ratio. Another important parameter is a proper oxygen and carbon dioxide transfer, associated to a proper mixing of the culture, which also facilitates a homogeneous light exposure and avoid biomass deposition or creation of biofilm (Płaczek *et al.* 2017).

Tubular reactors are a common design for large outdoor facilities, which can be found in different orientations: horizontal tubes in a single plane, vertical parallel stacks of horizontal tubes, or even helically (Bahadar and Bilal Khan 2013; Figure 2). Despite the bigger investment costs, vertical stacks lead to higher productivities and photosynthetic efficiencies when compared to a horizontal single plane, due to higher light capture. The liquid velocity inside the tubes is usually around 0.5 ms^{-1} (De Vree *et al.* 2015) and the growth medium is circulated with an airlift device, in order to avoid mechanically stressing the cells with the pumps (Bahadar and Bilal Khan 2013). Despite the liquid's motion, fouling can occur when the reactor is run for long periods of time. The tubes are connected to a degasser or striper vessel, where the oxygen produced by photosynthesis is removed by air injection, in order to avoid photooxidation (De Vree *et al.* 2015). In a more recent design, instead of filling in the tubes entirely, a circulating overlayer of air is used as a technique to facilitate gas transfer within the culture (LGem).

Figure 2: Tubular photobioreactors, horizontally (on the left) and vertically (on the right) stacked, at AlgaePARC (Wageningen, Netherlands).

Flat panel photobioreactors are the ones with bigger superficial area to volume ratio, which reflects in a higher photosynthetic efficiency (Figure 3). The culture is mixed by aeration, which can have clogging issues when operated for long periods of time (De Vree *et al.* 2015). Other disadvantages are the formation of biofilm by some alga species when under hydromechanical stress, how it requires the use of several modules for a large-scale production (Płaczek *et al.* 2017) and has higher investment costs than tubular reactors (De Vree *et al.* 2015). At lab scale however, it has the advantage of offering a modular design, which can be tuned for the user's needs.

Figure 3: Flat panel photobioreactors at AlgaePARC (Wageningen, Netherlands) on the left, and at Necton (Olhão, Portugal) on the right.

Fermenter type photobioreactors can also be used (Figure 4). A very low superficial area to volume ratio leads to low productivities, but it's a robust reactor easier to accommodate bigger productions than lab scale flat panel reactors (Płaczek *et al.* 2017).

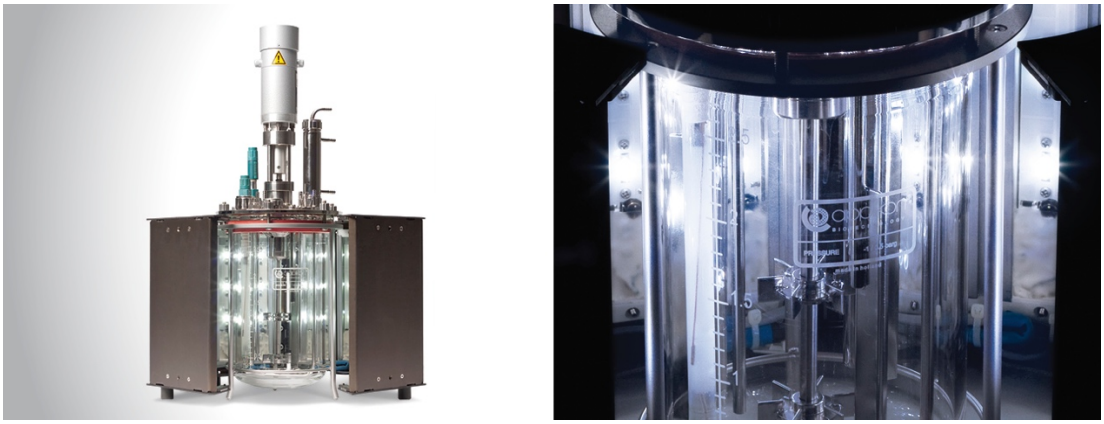

Figure 4: Fermenter type photobioreactor from Applikon ® Biotechnology (Applikon).

The reactors mentioned above are often built with materials such as Plexiglas, acrylic glass, PPMA or PVC, amongst others, depending on the expected lifetime of the set-up. In certain situations, polyethylene bags and sleeves are an attractive option due to its low cost and sterility, which can be kept in a stiff metal frame or hanging from an upper support. However, it should not be kept for long periods of time due to the material's deterioration and it's not the most sustainable alternative as it is a disposable reactor. In scaled up systems, temperature can be controlled either by the use of water sprinkles, by adding a coil to the degasser, or by installing the system inside a greenhouse (Płaczek *et al.* 2017).

2.2. Microalgae Applications

Microalgae are a promising resource for various fields, from feed to pharmaceutical drugs and energy, given their rich composition and possibility for genetic manipulation.

Microalgae offer a wide range of bioactive substances, which makes them attractive as both food and health supplements. Some are currently being produced at commercial scale for this reason. Microalgae have protective substances against free radicals to prevent from oxidative stress, such as carotenoids, which can be used in nutraceuticals and food. Carotenoids are therapeutic in oxidative stress-related diseases and consequent complications, such as diabetes, cancer, obesity or strokes (Khan *et al.* 2018). Phycocyanin, ß-carotene and astaxanthin are amongst the most important carotenoids synthetized by algae. *Dunaliella salina* is a known source for ß-carotene, given that it represents 10 to 14% of its dry weight. ß-carotene protects the membrane lipids from peroxidation, a phenomenon associated to diseases such as cancer, cardiovascular disease, Parkinson and atherosclerosis. Phenolic compounds and other vitamins also have strong antioxidant activities. Sterols are also interesting health promoting substances, for its hypo-cholesterolemia, anticancer and anti-inflammatory effects, as well as action against neurological diseases, such as Parkinson. There are several proteins and amino acids which are required for human cells to undergo their daily activities, but not all can be naturally synthetized and need to be acquired in the diet. Microalgae have many essential amino acids, and their proteins reduce cholesterol levels by activating cholecystokinin. A more specific example could be the protein cyanovirin, produced by *Nostoc*, which has an antiviral action against HIV and influenza virus (Khan *et al.* 2018). Another important commercial product with high therapeutic value is polyunsaturated fatty acids. Omega-3 and omega-6 fatty acids are fundamental for the human body, even though humans cannot produce them, meaning they should be present as a dietary supplement. They guard membrane integrity, delay aging, supress cholesterol levels and prevent cardiovascular diseases. Eicosapentaenoic acid (EPA) and docosahexaenoic acid (DHA) are two of the most relevant omega-3 fatty acids for human health and both can be found in several species of microalgae. In fact, microalgae are the only alternative to fish oils, whose availability is limited and currently unable to satisfy the current demand of EPA and DHA. Some microalgae have been genetically modified in order to enhance their EPA and DHA content quite successfully, making this process feasible at a commercial scale. Several microalgae species produce also toxic substances, which can be lethal to humans and animals. However, used in a controlled manner these toxins can be interesting for its antibacterial and antifungal activities. Moreover, some studies found cyanotoxins can be used for treating tumours (Khan *et al.* 2018). As we can see, the pharmaceutical market is one of the biggest for microalgae.

Something worth mentioning is how microalgae do not produce some important metabolites, or produce them in significantly smaller quantities, under normal conditions. Some compounds, such as storage compounds, are only accumulated in the cell under stress conditions, such as nitrogen deprivation, high temperature, light or salinity, amongst others. It so happens because the production of these compounds is a defence mechanism from the cell, triggered by adverse conditions (Khan *et al.* 2018).

Given their high nutritional value and beneficial components, microalgae are appealing for both food and feed industries. Whilst only a few species of microalgae are approved for human consumption, there is a wide variety of microalgae currently being produced for feed, mostly for aquaculture hatcheries for

fish, shrimps, shellfish larviculture, live-prey cultivation or even home aquariums (Phytobloom). Algal biomass is considered to enhance the growth performances and disease resistance of edible fishes, besides improving the skin and flesh colour of some fishes (Roy and Pal 2015). In aquaculture, microalgae are also used to induce Green Water Technique in fish tanks, which has a positive effect on the larvae fish growth and survival since it generates an environment closer to the natural one, besides improving the water quality from the tanks (Phytobloom).

Another promising application of microalgae is biofuels, such as bioethanol, biodiesel or hydrogen. The worldwide liquid fuels demand is predicted to increase continuously in the following decades (Laurens 2017), however, one knows continuing to use fossil fuels for so long is not a viable option due its negative environmental impact. The dependency on fossil fuels also brings political and economic instability, as many countries are still dependent on imported fossil fuels, mostly for transportation (Laurens 2017). Liquid fuels, as any renewable energy, offer the possibility of self-independence, energy-wise. On the other hand, the price of petroleum has fallen by 50% from 2014 to 2017, which increases the concerns and challenges of producing competitive pricing biofuels (Laurens 2017). Agricultural crops can be used for biofuels production, however there is a high demand for food sources, which have a higher price than fuels. First generation fuels have a strong competition, not only economically but also social and ethically. Second generation biofuels use agricultural and forestry waste as raw material, however there is usually lack of resources at a local level to sustain an economically feasible production. This leads to waste importation and transportation, which might be counterproductive if one looks at the overall carbon footprint of the process (Islam *et al.* 2017). Microalgae are an appealing alternative, since they don't require the usage of arable land or fresh water, their photosynthetic conversion efficiency is considerably higher than the one from terrestrial crops (Laurens 2017) and they have the possibility to grow on sequestered CO_2 (Khan *et al.* 2018).

Microalgae are considered one of the most promising sources for biodiesel given their high fatty acids content, which can go from 5 to 77 wt% depending on the specie and growth conditions (Halim *et al.* 2012). The fatty acid profile of a microalgae also depends on the specie and its life conditions, as well as the moment from its life cycle when they are harvested (Dunstan *et al.* 1993). Lipids can be divided into two groups: storage/neutral or structural/polar lipids. As the name suggests, structural lipids are the ones which form the bilayer cell membranes, while storage lipids, such as triacylglycerols (TAG) are mostly used for energy storage. Although both of them can be trans-esterified into biodiesel, the polar lipids content from some species is quite rich in polyunsaturated fatty acids with more than four double bounds, which needs to be under a certain value according to the European standards for biofuel. The iodine value of this oil is indeed higher than permitted, which also translates into lower cetane number and combustibility. For this reason, one should focus on microalgae's neutral lipids for third generation biodiesel production (Islam *et al.* 2017). Inducing stress conditions before harvesting by nitrogen deprivation is a commonly used technique to increase the neutral lipids content inside the cells. Research is being carried out on genetically engineered strains with higher lipid content and tuned fatty acids profiles.

Nowadays, the use of microalgae for biodiesel production alone, is still considered not to be economically feasible, and there are no production facilities at commercial scale for this end-use. One

of the biggest challenges which leads to this scenario, is the lipid extraction from the cells. Currently there are several different extraction approaches, such as mechanical disruption, ultrasonic-assisted extraction, solvent extraction, supercritical fluid extraction or thermo-chemical liquefaction. To be noticed that mechanical disruption and solvent extraction demand pre-treatment of the biomass, namely dewatering and drying, which are energy consuming activities. Mechanical disruption includes methods such as bead milling or mechanical pressing, which rely on the physical damage of the cell wall by shear stress or crushing. Ultrasonic-assisted extraction relies on submitting the cells to sound waves, which assist on their contents release. Solvent extraction makes use of organic solvents, to which the lipids migrate due to higher solubility and affinity than to the aqueous phase. The most commonly used solvent is hexane, due to its low cost, availability, density and boiling point, but others such as benzene, iso-propanol or ethanol can also be used. When combined to higher temperature and pressure it is referred to as Accelerated Solvent extraction (ASE) which not only allows for a bigger lipids recovery but can also be applied to wet biomass. Despite its high efficiency, solvent extraction is not an environmentally friendly option due to the use of toxic substances. Supercritical fluid extraction uses, as the name suggests, a fluid submitted to temperature and pressure above its critical point, which allows it to better penetrate the cell, decreasing the extraction time and increasing the yield. Carbon dioxide is the most common choice due to low critical temperature and pressure, chemical inertness and availability (Islam *et al.* 2017). An appealing alternative is the use of supercritical methanol in a direct trans-esterification, meaning the lipids are extracted and trans-esterified in one single process (Halim *et al.* 2012). Although it avoids the use of toxic solvents and has a high recovery efficiency, its high capital costs and energy consumption are strong limitations to this method. One of the most interesting thermo-chemical liquefaction processes is hydrothermal liquefaction (HTL), which converts the biomass into bio-crude under mild temperature and pressure. A two steps HTL can be performed, first step at mild conditions and second with more aggressive environment, in order to prevent a high amount of nitrogen in the bio-crude, which brings complications to the refinement and lowers the fuel quality. With this set up, more valuable products can also be extracted in the first step, increasing the benefits from the process. HTL is highly energy efficient and promising, yet it is still in an early stage of development (Islam *et al.* 2017).
Biodiesel can be used in diesel engines, although it has a lower power output and torque due to lower high heating value (HHV). On average, biodiesel's HHV is 10% lower than the one of diesel, because of the presence of unsaturated hydrocarbon, shorter length chains and higher oxygen content. For these same reasons, microalgae biodiesel usually has a lower HHV than biodiesel from other sources. Burning microalgae biodiesel leads to a significant reduction on exhaust emissions from CO, HC or particulate matter, and to an increase on NOx emissions, generally speaking. One must notice the small amount of research made on this area, and that there are records of reduced NOx emissions both from microalgae biodiesel and a blend between it, ethanol and petroleum diesel (Islam *et al.* 2017).
Bioethanol is currently one of the mostly used and cleanest biofuels. It has good properties as a fuel, such as a considerably high octane number, and its burning produces the least Greenhouse gas emissions. The world leaders in bioethanol production are USA and Brazil, which use corn and sugar as their main raw material, respectively. In the European Union, wheat and sugar beet are the most common sugar sources. Microalgae contain several different hydrocarbons, such as glycogen, starch

or cellulose, which can be easily converted into fermentable sugars. Those sugars will then be fermented into bioethanol, recurring to bacteria or yeast. Since they are usually substrate dependent, and the produced substrate will depend on the used microalgae strain and cultivation conditions, one must consider all these factors as a whole in order to maximize the production rates and yields. Originally, the microalgae content in hydrocarbons is not high enough for commercial production of bioethanol from microalgae, even when it is increased by induced stress conditions. Genetic engineering tools are allowing us to evolve towards a solution for this issue (Khan *et al.* 2018). An alternative way of producing bioethanol is using genetically enhanced cyanobacteria. These were modified to overexpress the genes for fermentation pathway enzymes, namely Pyruvate decarboxylase (PDC) and Alcohol dehydrogenase (ADH). The produced ethanol is secreted through the cell walls into the medium, not requiring the cells to be harvested nor destroyed (Algenol). Initially, the water and ethanol mixture were distilled, an energy consuming separation method (Luo *et al.* 2010). The photobioreactors were then improved in order to address this problem, by working in the same principle as salt-water purifiers, except here ethanol, and not water, was evaporating, condensing and being collected (Algenol). These photobioreactor design was made and patented by the company Algenol (Woods *et al.* 2012). The design was not their only concern, as they also had to select a strain which would resist both at the presence of ethanol 5% v/v and to temperatures up to 55°C (Legere *et al.* 2017).

Hydrogen is the most energy dense fuel, its combustion's only product is water and can be easily converted into electricity via fuel cells. Currently its main source are still fossil fuels, and even though it can be produced from water electrolysis using renewable energy sources, such as solar or wind, there is a substantial interest in finding alternative paths for its production. Microalgae can offer such an alternative. *C. reinhardtii* is considered the best eukaryotic cells for H_2 production, although there are some limitations that still need to be overcome. When growing phototrophically, the Photo System II (PS II) produces oxygen which inhibits the action of hydrogenases. For this reason, in order to enhance the H_2 production one can first grow the microalgae phototrophically and then promote an anaerobic phase with sulphur deprivation, in which acetate will be the main carbon source of the cell. Alternatives to that are the inhibition of the PS II or the removal of oxygen with N_2 bubbling. Genetic engineering is a tool which is helping to bypass such limitations, by increasing the hydrogenases' tolerance to O_2 or improving the metabolism of the cell under sulphur deprivation (Esquível *et al.* 2011).

Biogas can also be produced with microalgae, from the anaerobic digestion (AD) of the intact biomass. Their high energy content and low ash content make them a good feedstock for AD, although the yields are extremely strain dependent. For example, strains without cell walls or with protein-based walls, without cellulose nor hemicellulose, are easier to degrade. An interesting concept is the possibility of using the biomass remains after a lipid extraction for AD, although their C:N ratio is often too low for the process. One must assess it and choose appropriate microbes depending on that. Since it doesn't require a pure culture, the biomass source can be produced via cheaper methods and it can also be combined with wastewater treatment (Laurens 2017).

More recently, the thermochemical conversion from microalgae biomass has been gaining more attention, such as pyrolysis, torrefaction, gasification, combustion or hydrothermal liquefaction. A drawback from these processes is how they require biomass dewatering and pre-drying, apart from

hydrothermal liquefaction. In fact, torrefaction, which consists in a mild pyrolysis, is more commonly used as a biomass upgrading technique rather than as it leads to a more energetically dense product. Pyrolysis and hydrothermal liquefaction seem to be the most appealing methods due to the bio-oil they produce, which can be later on upgraded into a higher quality liquid fuel. Given the main focus on the pyrolysis bio-oil, rather than on biochar, fast pyrolysis is used and not slow pyrolysis, with or without catalysts. To be noticed that different strains lead to different high heating values, and that these processes are more often applied to low lipid content strains or to residues from high lipid content strains after lipid extraction (Kumar *et al.* 2017).

An interesting concept is the one of Microalgae biorefineries, which consists in the extraction and utilization of all potentially valuable components from the cell for different end-users. It usually comprises bio-based products and bioenergy applications, for example, pigments would be removed for pharmaceutics or cosmetics, proteins for aquaculture and fatty acids for bio-diesel production. In this way, the revenue from the highest valuable products would compensate for the production of the lower market price products, with an overall economically feasible project.

Some microalgae species can also be used in wastewater treatment, such as municipal, industrial, agricultural or food processing wastewater. As the global population continues to increase and to have a higher quality of life, the generated waste is increasingly becoming one of the most important challenges from our societies, wastewater included. Nowadays, most plants remove the nitrogen and convert it to N_2, before releasing it to the atmosphere. Phosphorus is precipitated with cations such as calcium or aluminium, which is a costly removal process. Microalgae is not only an alternative process for the removal from these nutrients, but also a way of utilizing waste for making valuable products. On the other hand, the production of the microalgae and their outcomes will be cheaper as the most fundamental nutrients for the biomass growth come from the waste stream. Some microalgae strains can remove heavy metals, pesticides, organic and inorganic toxins and even pathogens, by accumulating them and/or utilizing them in their cells. To be noticed that the efficiency from heavy metals removal and the tolerance to organic pollutants are strain dependent characteristics. Algae cultivation for wastewater treatment are most commonly open systems, such as raceway ponds or waste stabilization ponds (WSP). Waste stabilization ponds are similar to conventional oxidation ponds where both bacteria and algae grow to treat the waste. A limitation to these systems can be a deficit of CO_2 in comparison to the amounts of nitrogen and phosphorous available, which can be solved by sparging additional CO_2 to the cultures, eventually sequestering CO_2 (Molazadeh *et al.* 2019).

To conclude, microalgae have a huge range of possible applications and are a promising tool towards more sustainable alternatives for a variety of fields.

2.3. From *C. reinhardtii* to B1 and B2 strains

Chlamydomonas reinhardtii is a green flagellate, which was first isolated by G. M. Smith in 1945 in Massachusetts. Its simplicity, rapid growth and high biomass production at low cost (Neupert *et al.* 2009) was attractive, and by 1960s it had become the most widely studied species in laboratory work, being considered as the type species of the genus *Chlamydomonas* (Harris 1989). It's a freshwater alga that grows under both phototrophic and heterotrophic conditions, and therefor mixotrophically as well, and is capable of sexual reproduction (Gallaher *et al.* 2015). *Chlamydomonas reinhardtii* is considered the reference for microalgal metabolism (Klok *et al.* 2014), given the broad knowledge on this specie. All three genomes, nuclear, plastid and mitochondrial, have been sequenced and are easy to genetically modify, making it an appealing platform for genetic manipulations (Neupert *et al.* 2009). This combined with a large library of available mutants, facilitates further research and widens the span of its applications.

Short after it was isolated, three main lineages were created from what supposedly was a single zygospore collected by G. M. Smith. Later sequence analysis from these three lineages led to results inconsistent with this supposition, and the truth behind is still unclear. Either way, both lineages were well stablished and separated since early 1950s, and the main registered evolutions within each lineage can be seen in Figure 5. Although most strains from Sager and Cambridge lineages are able to uptake nitrates, two unlinked mutations *nit-1* and *nit-2* have been associated to the Eberson-Levine lineage since its beginning, either of which being sufficient to prevent nitrate utilization (Harris 1989). In 1970, D. R. Davies generated several cell-wall deficient mutants from Levine's wild type, with the goal of better understanding the cell-wall formation process in *C. reinhardtii*. The mutagenic agent N-methyl-N'-nitro-N-nitrosoguanidine was used, and the mutants *cw15* (Davies and Plaskitt 1971) and *cw92* (Hyams and Davies 1972), amongst others, were created. René F. Matagne developed extensive work on *C. reinhardtii* mutants to better understand its regulatory mechanisms, during which the strain CC-4350 cw15 nit1 nit2 arg7-8 mt+ was created. This strain is characterized by a high transformation efficiency and having no flagella (Chlamydomonas Resource Center).

There was something limiting the application of the promising *C. reinhardtii*: poor expression of foreign genes introduced in the nuclear genome. Additionally, if a transgene expression was observed, it would often be instable, meaning that it would be frequently lost later on for unknown reasons. This could be a defence mechanism from the cell against invading nucleic acid sequences from viruses or other pathogens, a hypothesis supported by the high resistance of Chlamydomonas against pathogenic infections. However, it was an obstacle for both basic and applied green algae research. Neupert *et al.* (2009) understood that if this was the result of a transgene suppression mechanism, it should be possible to isolate mutants where this mechanism was defective. With this in mind, they induced UV light mutagenesis in the cell wall-deficient CC-4350 (cw15 nit1 nit2 arg7–8 mt+ [Matagne 302]) strain and designed a screening process, from which one successful mutant with high heterologous expression was found: UVM4.

C. reinhardtii UVM4 culture was used by Lauersen *et al.* (2016) to produce genetically modified mutants capable of heterologous expression of terpene synthases, which would not only produce but also excrete the sesquiterpenoid to the surrounding medium. In a similar way, GMO strains were designed

by Lauersen *et al.* (2018) capable of heterologous expression of diterpene synthases and enzymes from the MEP pathway, leading to the production and excretion of 13R(+)Manoyl Oxide and its hydroxylated variant. The designation B1 was given to strain producing only 13R(+)Manoyl Oxide and B2 to the strain producing also 9-hydroxy-Manoyl Oxide. These were the strains used during this thesis.

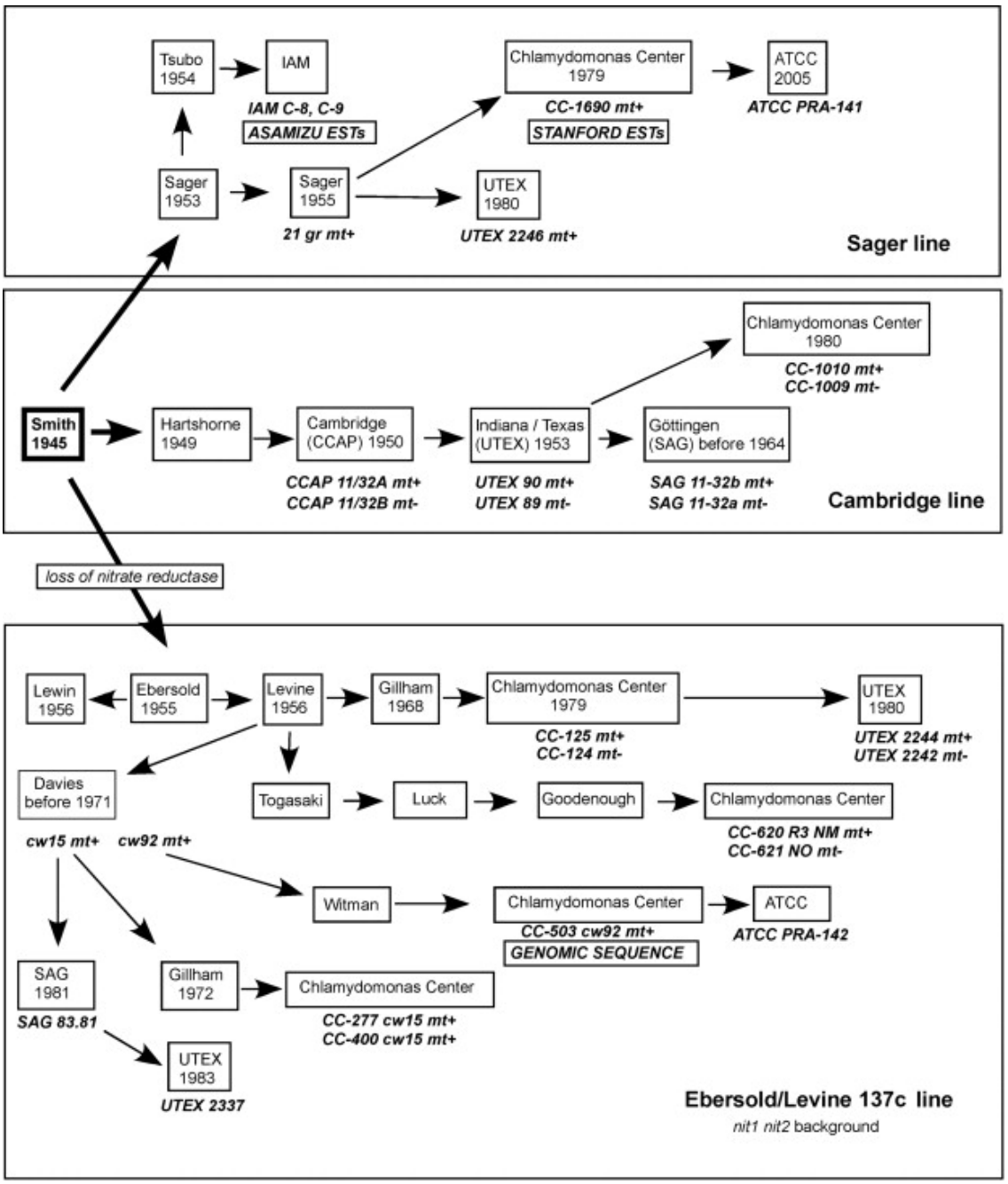

Figure 5: Main laboratory strains of C. reinhardtii, in Chlamydomonas Sourcebook (Harris 1989).

2.4. From Terpenoids to Forskolin

Terpenoids are a class of organic compounds commonly found in Nature. They derive from terpenes, a large class of hydrocarbons which can be broken down into isoprene units, by having additional functional groups which usually contain oxygen. There are more than 50 000 different terpenoids, constituting the largest class of plants metabolites (Dictionary of natural Products). In Nature, these compounds are usually associated to functions such as light reception, photoprotection or plant defence. In a human-made world however, they have an even broader range of applications, from medicines to food and feed additives, agricultural support, cosmetics, chemical building blocks and even biofuels (Lauersen *et al.* 2018).

Manoyl Oxide is a terpenoid particularly interesting for its potential in the medical field. Both 13R(+)Manoyl Oxide and its hydroxylated variant, 9-hydroxy-Manoyl Oxide, are precursors for Forskolin (Figure 6), which has anti-aging, antioxidant and anti-inflammatory properties. It is promising for heart and respiratory disorders, such as congestive heart failure, angina, or asthma, as well for glaucoma and some type of cancers (Khatun 2011). Additionally, it is commonly known for its weight-loss applications, although some claim lack of proper research in that area (Healthline).

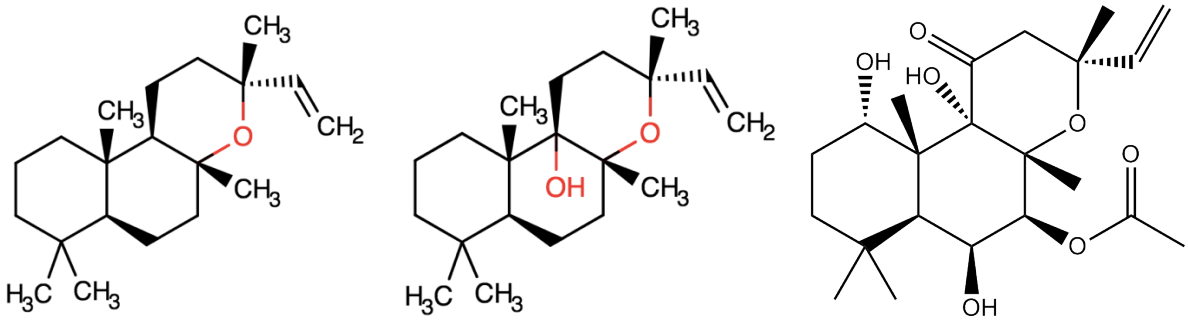

Figure 6: Chemical structure from Manoyl Oxide, 9-hydroxy-Manoyl Oxide (Chemicalize) *and forskolin (from left to right).*

Forskolin can be naturally found in the roots of the plant *Coleus forskohlii*, also known as *Plectranthus barbatus*, which has been extensively used in traditional medicine to treat some of the disorders mentioned above (Coleus). However, plants produce various types of diterpenoids each in small quantities, so if extracted it requires a demanding purification process and large amounts of biomass, leading to low yields. In this way, not only the process is expensive but also not eco-friendly. The existing chemical processes to synthetize this compound are still economically challenging, although recent advancements have been made (Pateraki *et al.* 2017). Currently the most promising alternatives are in the field of biotechnology. Ignea *et al.* (2016) were able to synthetize 11β-hydroxy-Manoyl Oxide, another forskolin precursor, using surrogate enzymatic activities in yeast (Ignea *et al.* 2016), while Guo *et al.* (2019) successfully produced 13R-Manoyl Oxide through metabolic engineering of *Saccharomyces cerevisiae*, a particular species of yeast (Guo *et al.* 2019). *Escherichia coli* strains have also been used to obtain Manoyl Oxide by *Nielsen et al.* (2014) (Nielsen *et al.* 2014). Although there are no known diterpene synthases native to microalgae, these can offer a more favourable environment for heterologous expression than fermentative microbes, given its temperature, chemical composition and

compartmentalization. More importantly, microalgae have a naturally high turnover of isoprenoids and of the precursor of both pigments and diterpenoids, geranylgeranyl pyrophosphate (GGPP) (Lauersen *et al*. 2018). For this, microalgae are an option worth exploring.

2.5. Terpenoids and Bioenergy

As previously mentioned, producing biodiesel from microalgae is still not economically feasible, and it relies either on toxic solvents or energy-demanding approaches. In the biotechnology field, the focus has been on creating genetically engineered strains with enhanced oil yields, as TAG secretion from the cells would go entirely against their normal metabolism, and so far, has not been achieved as for the author's knowledge. There are, however, currently several mutants which can excrete different products that can also be useful in the production of biodiesel. Kato *et al.* (2017) genetically engineered cyanobacteria, in order to produce and release free fatty acids into the medium. Another promising option is the production of terpenes, such as bisabolane, farnesene, cineole, amongst others.

Bisabolane has a carbon length close to the average one of biodiesel, as well as comparable cetane number. Its Derived Cetane Number (DCN) is 41.9, which is still in the 40 to 55 desirable range for standard diesel. It's non-corrosive, and its lower cloud point makes it a potential anticlouding additive for improving diesel fuels cold properties. More specifically, bisabolane has a cloud point of -78˚C, significantly lower than the one of diesel's, -35˚C, and even more than the one from commercial biodiesel's, -3˚C. Given its comparable energy density do D2-diesel, bisabolane can even be used as diesel or jet fuel alternative (Joint BioEnergy Institute). Through genetic engineering of *E. coli* and *S. cerevisiae*, the production of bisabolene via these microorganisms has been enhanced, which can then be converted to bisabolane via hydrogenation (Peralta-Yahya *et al.* 2011). In cyanobacteria the production of α-bisabolene has also been achieved, moreover, a dodecane layer was also applied in order to extract the product and avoiding product feedback inhibition (Davies *et al.* 2014). Microalgae have advantages over these microorganisms: when compared with fermentative microbes, they can grow only with natural light and carbon dioxide, compared with cyanobacteria they can achieve higher production yields. Lauersen *et al.* (2016) was able to demonstrate the heterologous expression of terpenoids in *C. reinhardtii*, which has a flexible metabolism with a high terpenoid turnover, after which Wichmann *et al.* (2018) was able to produce bisabolene with GMO strains from that same microalga. Harun *et al.* (2018) concluded that the bisabolene production through genetically modified *C. reinhardtii* is light intensity independent, but differs with temperature, plus she theoretically predicted that a continuous production and scale up is possible. In the mentioned experiments, a dodecane layer was added in order to enhance the terpenoid's production, since it would avoid the feedback inhibition.

Farnesene can also be further hydrogenized into an alkane, farnesane, which has comparable density, viscosity, specific heat and cetane number to diesel fuel. Engine performance tests with farnesane led to similar results to the ones with diesel, with a small power decrease and reduced emissions (Holmborn 2015). Farnesene is then considered a promising precursor of diesel or jet fuel (Gupta and Phulara 2015), in fact, a blend with 10% farnesane was already used in commercial flights in 2014 (Biofuels Digest). It is currently being produced at a commercial scale via genetically engineered *S. cerevisiae*, which demands sugar cane plantations to produce the yeast's feedstock (Farnesene net). It has also

been produced by genetically modified strains of *E. coli* and cyanobacteria *Anabaena* sp., the latest having the advantage of using CO_2 as carbon source (Gupta and Phulara 2015). Cineole has been produced by genetically modified red yeast *R. toruloides* (Zhuang *et al.* 2019). When blended up to 80%(v/v) with gasoline, the resulting fuel has an octane number of 95, and at a 20% ratio with Jet-A, there are no significant changes on the fuel property. If added in a 10% (v/v) fraction to ultra-low diesel, it improves its cold filter plugging point, cetane number and oxidative stability. That being said, cineole is a potential additive for many different and broadly used liquid fuels (Strobel 2015). Monoterpenes such as α-pinene, camphene or limonene are also considered possible raw materials for jet fuel (Gupta and Phulara 2015).

To conclude, there are many different terpenes and terpenoids with valuable applications in the energy field, which would benefit from further advancements on their production processes.

2.6. Terpenoids continuous in situ extraction

To assure a continuous process, one must extract the compound of interest without compromising the viability of the cells. Hejazi *et al.* (2002) studied the continuous in situ carotenoids extraction from *D. salina*, first of their knowledge to extracting carotenoids without intentionally destroying the cells. The concept of simultaneously producing and extracting a product at a constant biomass concentration is nicknamed “milking”. The extraction solvent used was dodecane, a commonly used solvent for terpenoid extraction, given their high affinity to the solvent and the solvent’s low solubility in water. Kleinegris *et al.* (2010) noticed *D. salina* cells uptake dodecane, which is responsible for morphological changes and increased activity of the cell membrane. For this reason, direct contact between the cells and the organic solvent is not a necessity but increases the efficiency of the process. The ß-carotene would then exit the cell either by diffusion or exocytosis. The microalgae were first grown in batch in a flat panel photobioreactor and then stressed to promote carotenoids accumulation. In order to extract the carotenoids, the microalgae were placed in a vessel with a dodecane overlayer, where dodecane was also being sparged from the bottom. The enhanced contact between the cells and the dodecane molecules due to its sparging considerably increased the cell death rate. Additionally, the aeration caused the sparged dodecane to emulsify and spread through the whole vessel (Kleinegris 2010).

de Boeck (2019) analysed the extraction of Manoyl Oxide from both B1 and B2 strains with different organic solvents, namely hexane, octane, decane, dodecane, tetradecane and hexadecane. The logarithm of the partition coefficient for the mixture of octanol and water ($\log P_{o/w}$) is an indicator of hydrophobicity. The lower it is the more soluble in water the compound is, and therefore the more toxic it is for microorganisms, as it needs to be higher than 5 for the solvent to be biocompatible (Laane, Hilhorst, and Veeger 1987). For this particular case, it was seen that $\log P_{o/w}$ should be higher than 6, meaning that the first three solvents were too toxic for the microalgae. It was concluded dodecane was the best option when considering both the extraction capacity and the cells viability (Boeck 2019). A potential alternative is isopropyl myristate (Lauersen *et al.* 2018), successfully used for the extraction of monoterpenes in different systems (Biotechnology for biofuels) and with a $\log P_{o/w}$ of 7.3 (The Good Scents company).

The possibility of using XAD-4 resins has also been examined for the system in study. Given the low solubility of these terpenoids in water (Chemicalize) and the hydrophobicity of the resins (Sigma Aldrich), these are able to adsorb them, thus extracting them from the medium. Further research is still needed for the improvement of this extraction method, however, it has proven that no direct contact between an organic solvent and the *C. reinhardtii* GMO strains is required (Lanting 2019).

3. Materials and Methods

3.1. Strains and Cultivation Conditions

Two genetically modified strains from *C. reinhardtii* were used, here mentioned as B1 and B2. B1 produces Manoyl Oxide, whilst B2 produces both Manoyl Oxide and its hydroxylated variant, 9-hydroxy-Manoyl Oxide. B1 was only used on the first experiment, after which it was decided to focus only on the B2 strain.

The maintenance cultures were inoculated in Tris-Acetate-Phosphate (TAP) Medium (Gorman and Levine 1965, Annex 1) and kept in a shake incubator at 25°C with 0.2% CO_2 and 150 μE of light intensity in a 16:8 day-night cycle. During the experiments, 2% CO_2, a higher light intensity and different medium were used. More details for the conditions varying from experiment to experiment can be found in the sections below. To be noticed that the nitrogen source was Ammonium Chloride, given that the used strains cannot uptake nitrates (Lauersen *et al.* 2018).

3.2. Optical Density and Dry weight calibration

In order to assess the cultures' growth, optical density (OD) was measured on a daily basis during all experiments. It was measured at three different wavelengths: 480 nm for carotenoids, 680 nm for chlorophyll A and 750 nm for the overall turbidity of the sample (Griffiths *et al.* 2011). If the optical density registered at 680 nm is higher than the one at 750 nm it can be assumed the sample's turbidity is mostly due to microalgae and no significant contamination is taking place. Further on, all mentions to the OD refer to the OD measured at 750 nm.

Initially, dry weight measurements were performed by filtering diluted culture samples with GF/F (nominal pore size 0.7 μm) filters and washing them with ammonium formate 0.5M, followed by drying overnight at 100 °C until constant weight. Filters were allowed to cool down in desiccators with dried silica before weighting on an analytical scale. From those results, the biomass concentration was then calculated. A correlation between the OD and the biomass concentration of a set of samples was stablished, which is translated into the 1. More information about this can be found in Annex .

$$x\ (g/L) = 0{,}4592 \cdot OD(750\ nm) \qquad 1$$

3.3. Algaebator

The *Algaebator* is a small incubator specifically designed for microalgae, where they were kept in 250 mL Erlenmeyer flasks with around 100 mL of culture (Figure 7). The strains were initially kept at 150 μE, which was increased to 318 μE after two days. During the first experiment, the light was kept at 318 μE, on the second experiment it was increased to 636 μE after one day. The value 636 μE was chosen since it represents the average Dutch summer light in block (Benvenuti 2016), and 318 μE for being half of it. The mixture of the culture was assured by using magnetic stirrers. After one day in the incubator, a 10 mL dodecane overlayer was added to the flasks, which represented 10% (v/v) in the first

experiment and 8.3% (v/v) in the second one, ratios based on the protocol provided by Lauersen *et al.* (2018). In both runs, there were Erlenmeyers left without a dodecane layer, as controls. Daily samples from the cultures were taken for optical density determination, alongside with dodecane samples for Gas Chromatography with Flame Ionization Detector (GC-FID) analysis. On the second experiment, additional samples were taken to analyse the Manoyl Oxide content in the medium and inside the cells, whose procedure is described in Annex .

Figure 7: B1 and B2 strains in Erlenmeyer flasks in the Algaebator.

3.4. Algaemist Reactors

Algaemist is a flat panel photobioreactor with a capacity of 400 mL of culture and a 14 mm light path (Figure 8). Adjacent to the growth chamber there's a water jacket, which assures the culture to remain at the desired temperature. It is equipped with primary and secondary light sensors, along with temperature and pH probes holders. The sensors and probes communicate with the computer, allowing for online control from these parameters. The culture mixture is assured by the airflow, which is wetted before entering the reactor in order to prevent water loss inside the reactor (Breuer *et al.* 2013; Mooij 2012).

The system can be run in batch, semi-continuous or continuous, depending on if and how the operator controls it. The reactor can be run continuously in turbidostat mode, in which the secondary light is set at a desired level and the medium pump is activated every time it drops below the set point, in another words, every time the biomass grows above the desired concentration (Mooij 2012).

The *Algaemist* reactors were originally designed to control the pH with CO_2 addition. When the nitrogen source are nitrates, the culture will become more alkaline with the consumption of nitrates, which can be balanced by the addition of CO_2 and its shift to bicarbonate. However, when the nitrogen source is ammonium, its consumption increases the acidity of the medium and the pH needs to be controlled with base addition. For this reason, the *Algaemist* had to be connected to an external pump, which would turn on every time the pH would drop below the set point.

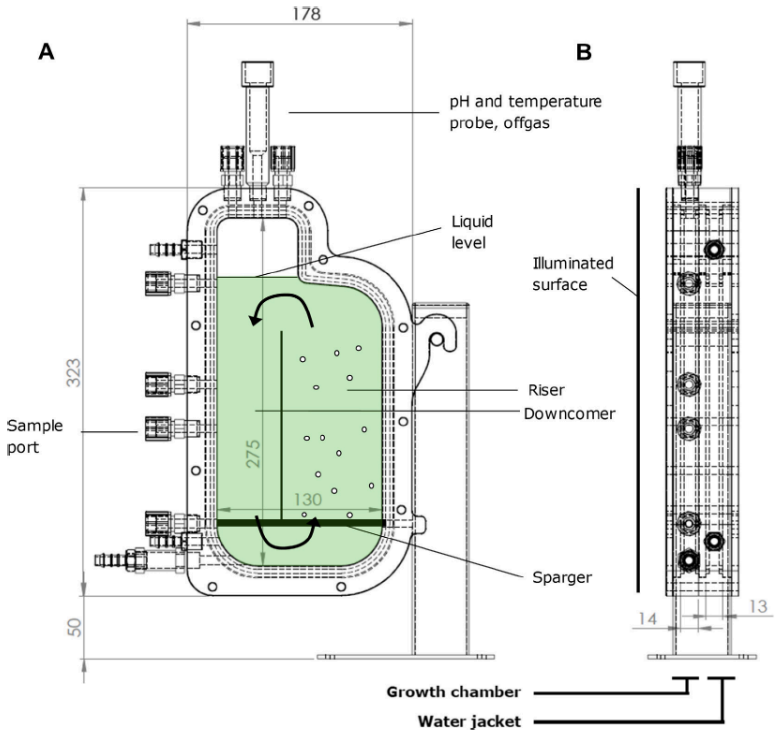

Figure 8: Frontal and side views of an Algaemist reactor (Breuer *et al*. 2013).

The cultures were kept at 25°C, a pH of 7.2 and an airflow of 200 mL/min with 2% CO_2. The light regime was a 16:8 day-night cycle, initially at 150 μE and later at 318 μE. TP Medium was used (**Erro! A origem d a referência não foi encontrada.**), a variant of TAP Medium with HCl 1M instead of Acetic Acid, in order to decrease the contamination risk in the reactor. Additionally, higher titres of Manoyl Oxide were obtained with CO_2 and 16:8 day-night cycles in comparison to other carbon sources and light regimes (Lauersen *et al.* 2018). The microalgae grew in batch until the desired optical density was reached, around 1.5. At that moment the turbidostat mode was activated and after one day under turbidostat the extraction system was turned on. Once the full content of the reactor had been renewed three times, or in another words, once 1200 mL of fresh medium had been added to the reactor, the turbidostat pump was turned off so that the culture would grow to a higher concentration, and then turned on again at an OD of 3. During this time, the extraction system was always turned on.

Just like before, the culture growth assessment was based on daily optical density analysis and the Manoyl Oxide production on GC-FID analysis from dodecane daily samples.

3.5. Infor Reactors

Infor is a flat panel photobioreactor with 2L capacity and 20 mm light path (Figure 9). The reactor's structure and operating modes are similar to the *Algaemist*, however there are some differences worth being highlighted (Klok 2013). The reactor is equipped with a condenser, which prevents water loss from evaporation. In order to avoid pressure build up inside the reactor, an air lock and a water lock are employed. The air lock is the normal air outlet after it passes through the condenser, while the water lock is a pressure stabilizer, in the form of a water manometer, and in last resource an emergency exit.

In case the algae would foam excessively, a 1%v/v aqueous solution of antifoam B under continuous stirring was connected to a pump, which would be manually activated in case of need.

The reactor was controlled in two different ways, depending on the situation: turbidostat and luminostat. In luminostat mode, the user sets the secondary light at the desired level. As the biomass grows, the computer will gradually increase the primary light in order to keep the secondary light constant. This assures the biomass has the optimal light per cell during its growth, and for that it can be a good alternative to a normal batch growth.

Two runs were performed with two *Infor* reactors each. In both runs, cultures were kept at 25°C, a pH of 7.2, an airflow of 1L/min with 2% CO_2 and a 16:8 day-night cycle. T2P 2N Medium was used (**Erro! A origem da referência não foi encontrada.**), a variant of TP Medium with twice the amount of phosphate and nitrogen, to allow the biomass to reach higher densities. In the first run, the microalgae grew in batch until reaching the desired biomass concentration, during which the light intensity was gradually manually increased, from 50 μE to 636 μE. In the second run, the biomass was grown under luminostat mode with 50 μE of outgoing light, being that the control mode was switched to turbidostat with 636 μE of ingoing light in one reactor and 2815 μE in the other. Once again, the extraction system was started after one day in turbidostat, and the light was reduced to 1877 μE in the reactor with the highest light intensity at this point. Just like before, optical density measurements were used to analyse the cultures' evolution. The Manoyl Oxide content in the dodecane, aqueous phase and inside the cells was investigated, and the protocol for the last two can be found on Annex .

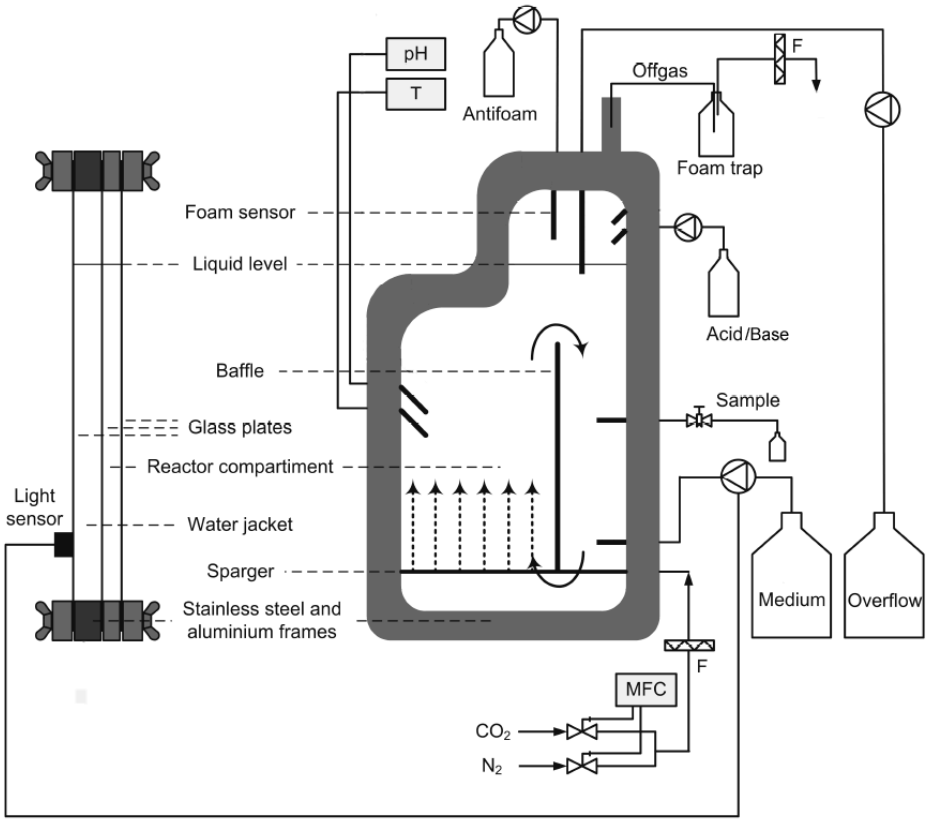

Figure 9: Frontal and side views of an Infor reactor (Klok 2013).

3.6. Extraction system

One of the focus of this thesis was on building and improving an extraction system which would work continuously. The reactor would be connected to an extraction vessel, so that the microalgae would be constantly circulating from the reactor into the extraction vessel and back to the reactor again (Figure 10 & Figure 11). A pump was needed to assure the flow and control its speed, both in and out the extraction vessel. Silicone tubes with 1.5 mm of internal diameter would transport the culture between the two vessels, and Watson-Marlow Marprene tubes with 1.42 mm internal diameter were used for the pump. A Watson-Marlow multi-channel peristaltic pump was used, model 205 U, at 90 rpm. Each path was split into two channels in the pump, which means that each path had actually two of the pump's channels working in parallel. The extraction vessel was a Schott Duran ® bottle whose lid had been modified to include the medium inlet and outlet and a sample port. In the experiment with the *Algaemist* a 250 mL Schott bottle was used, with 100 mL of culture and 50 mL of dodecane. For the *Infor* experiments a 500 mL bottle with 200 mL of culture and 100 mL of dodecane was utilized, to compensate for the larger reactor volume. The medium drops would fall from the top of the Schott bottle, cross the dodecane overlay and eventually burst into the medium underneath, which was under continuous stirring. After approximately 10 minutes for the *Algaemist* and 13 minutes for the *Infor*, those same microalgae cells would be sucked by the pump back into the reactor.

One of the main concerns while building up the set up was to assure the flow inside the tubes would be high enough, so that no biomass deposition would occur. During the system's operation, one should be particularly careful with the tuning of the pump, so that the rate at which the medium entered the extraction vessel was the same at which it exited, and the liquid levels inside the vessel and the reactor would remain the same.

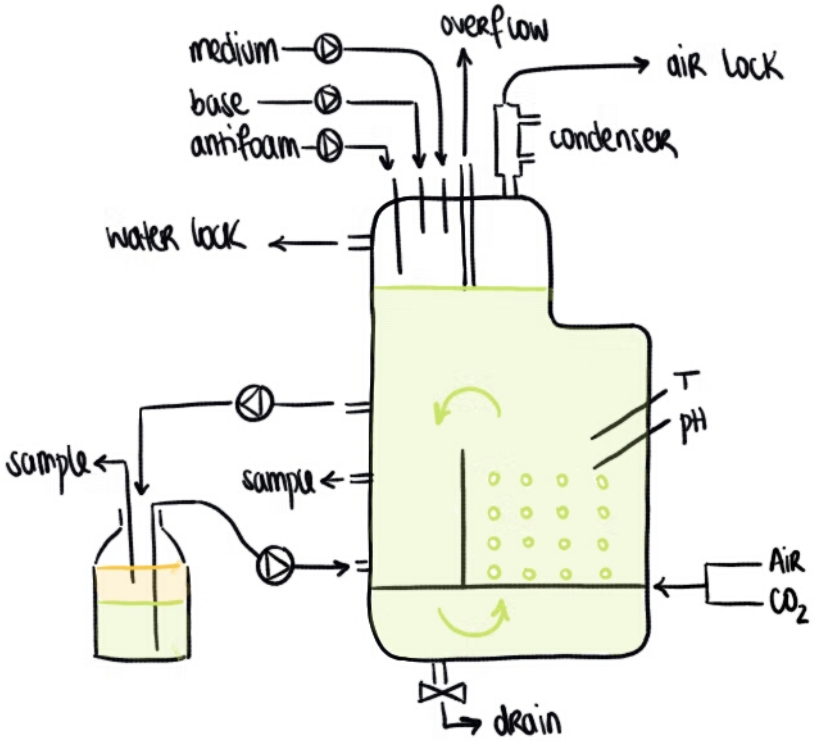

Figure 10: Schematic of the designed set-up applied for the Infor reactors.

Figure 11: Set-up during the experiments with Infor reactors. Underneath the bench there is the overflow bottle on the left and the fresh medium vessel on the right, on the scale. On the right side of the reactor the antifoam and the base bottles can be seen, the latest on a scale. In front of the reactor there is the water lock. The extraction vessel and pump are on the left side of the reactor. To be noticed that the reactor surface would usually be covered, so that the only incident light was from the LEDs.

3.7. Cell viability

The cell viability was assessed both right before the extraction system was turned on and at the end of the experiment, so that the death rate of the cells due to the proposed system could be understood. To do so, the method suggested by de Boeck (2019) for this particular strain was used, which consisted in dying the samples with Erythrosine B and counting the cells with a Neubauer chamber. Erythrosine B can only penetrate the non-viable cells, which gain a pink coloration and can easily be distinguished under the microscope. A more detailed description of the used protocol can be found in Annex .

3.8. Manoyl Oxide quantification

The concentration of Manoyl Oxide in the dodecane was determined using on a GC-FID 7890A from Agilent using a RESTEK Rxi-5ms column 0.25 µm (5% diphenyl, 95% dimethylpolysiloxane). Using a set of samples with a known Manoyl Oxide concentration provided by University of Bielefeld, a calibration line relating the peak's area shown in the used GC-FID to the Manoyl Oxide concentration was made. This relation is given by 2. The temperature programme employed by the GC-FID and further information on the calibration line can be found in Annex . Some samples were also sent to the University of Bielefeld to be analysed on the Gas Chromatography – Mass Spectrometry (GC-MS), following the procedure described in Lauersen *et al*. (2016).

$$m_{MO}\ (mg/L) = 0{,}2663 \cdot Area \qquad 2$$

4. Results and Discussion

4.1. Strains Evaluation

4.1.1. Comparison between B1 and B2 strains

The aim of this experiment was to compare the growth and terpenoid production rates of both strains. To do so, B1 and B2 were grown under similar conditions, and both the optical density and Manoyl Oxide concentration in the dodecane was measured on a daily basis, which can be seen in the graphs bellow. By day 4, the growth curve shifts to a stationary phase, indicating that the microalgae were nitrogen limited at an OD between 3 and 4 (Figure 12). This was corroborated by comparing the achieved biomass concentration with the initial amount of available nitrogen in the medium, considering it represents 6,3% (w/w) of the total biomass (Boyle and Morgan 2009).

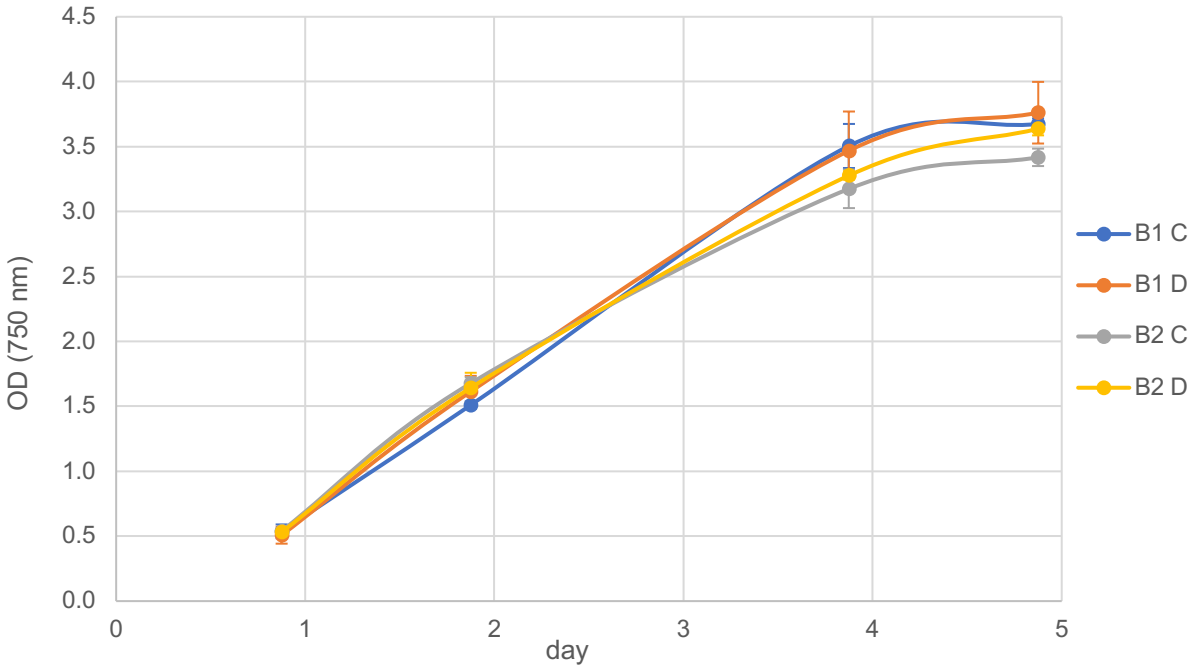

Figure 12: Optical density from both B1 and B2 strains in the algaebator. For each strain there were two controls (C) and four Erlenmeyers with a dodecane overlayer (D). Day zero is the day of the inoculation of the Erlenmeyers.

It can be observed that both strains lead to similar MO titters and growth rate (Figure 12 & Figure 13). As expected, the hydroxylated form was detected only in the samples from the B2 strain (Figure 14), however the terpenoid mostly produced by this strain was still Manoyl Oxide. This can be explained by looking at the production mechanism from this terpenoid, since MO is converted into 9OH-MO by a cytochrome enzyme located in the chloroplast's membrane (Lauersen *et al.* 2018). The large deviations observed for the 9OH-MO samples were most likely due to the operator's inexperience when the experiment was made. Given the similar behaviours of both strains and that 9OH-MO is a compound of bigger interest than MO, the following experiences were all carried out only with the B2 strain.

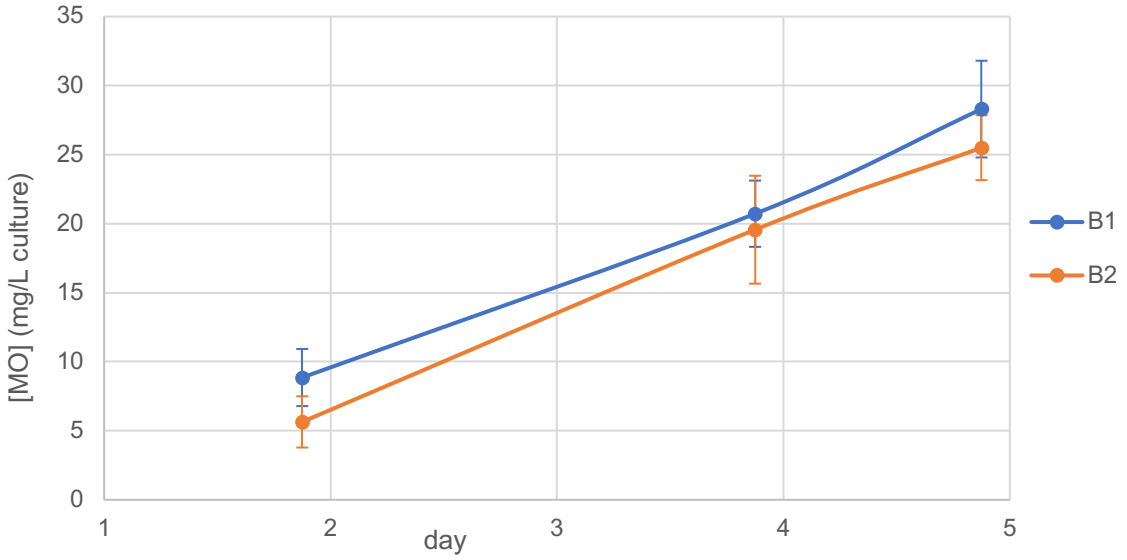

Figure 13: Manoyl Oxide concentration in mg per L of culture. Day zero is the day of the inoculation of the Erlenmeyers. The dodecane was introduced at day one.

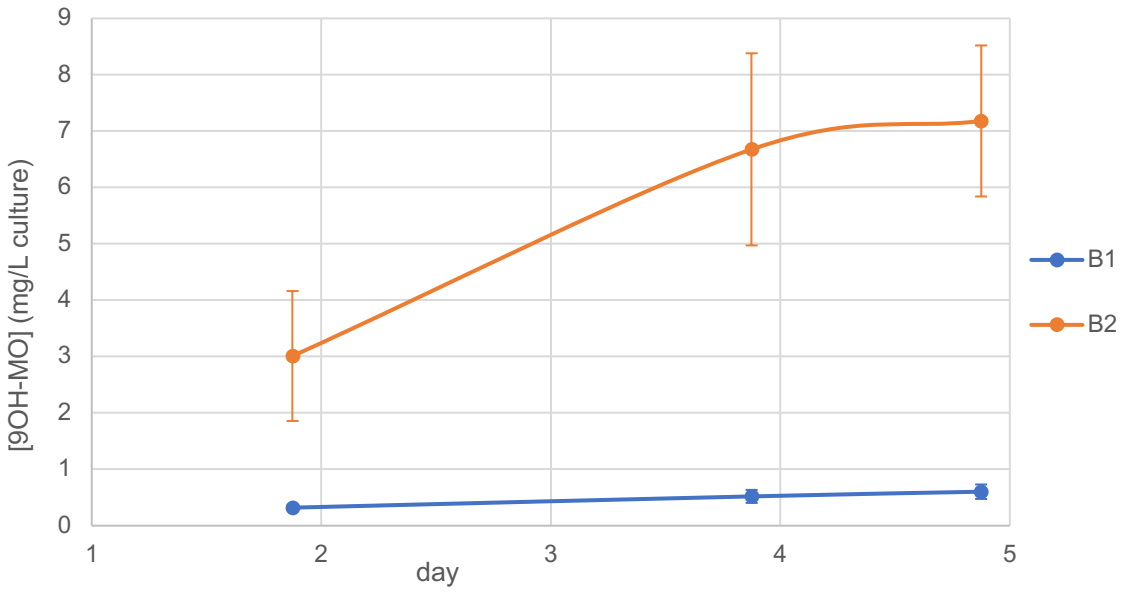

Figure 14: 9-hydroxy-Manoyl Oxide concentration in mg per L of culture. Day zero is the day of the inoculation of the Erlenmeyers. The dodecane was introduced at day one.

4.1.2. Effect of Light intensity

A second experience was performed with the aim of assessing the microalgae's response to higher light intensities and the effect of light on the respective productivities. The followed methodology was similar to the one of the first experiment, this time only with the B2 strain and a maximum light intensity of 636 µE. There were two different inoculation moments: the Erlenmeyer flasks where dodecane was added were inoculated several days before the ones which grew without any solvent layer throughout the whole experiment. The growth curves and terpenoids extraction from both this experiment and B2 samples from the previous one can be seen in Figure 15 to Figure 16.

From day 3 to day 4 the algae in contact with dodecane had no CO_2 and the temperature rose to almost 30°C due to a not well closed lid, which explains the flattening of the growth curve in that period. Due to this delay, the stationary phase was reached only at day 6, with an OD between 4.0 and 4.5. In Figure 15, both the real and corrected curves for these samples are presented.

Although the same cannot be observed in **Erro! A origem da referência não foi encontrada.**, the c oncentration of Manoyl Oxide in the medium suffered a small decrease during this time, which indicates that the lack of CO_2 also influenced the Manoyl Oxide production from the algae. This decrease is, however, considerably small when compared to the increase in Manoyl Oxide in the dodecane, which means the absence of CO_2 impacted the cells growth more than the terpenoid production. Given that there was acetic acid in the medium, this must have been the carbon and energy source of the produced Manoyl Oxide during this period, and it is curious to notice that the cells canalized the carbon substrate to produce the terpenoid instead of biomass. When analysing the terpenoids' production per mass of dry biomass (Figure 17), it can be seen that it decreased once the CO_2 was restored. After this drop, the rate remained lower than what it was in the first days. A decrease in terpenoid's productivity per mass of dry biomass throughout the experiment was also observed in the previous one and is an indication that the higher the biomass concentration, the lower is the productivity per mass of biomass, something which will be corroborated in section 4.4.

Regarding the comparison between lower and higher light intensities, as nitrogen limitation was reached before the biomass concentration was high enough to cause light limitation, and as the microalgae showed no light sensitivity up to 636 µE, no significant differences were seen between the two light intensities.

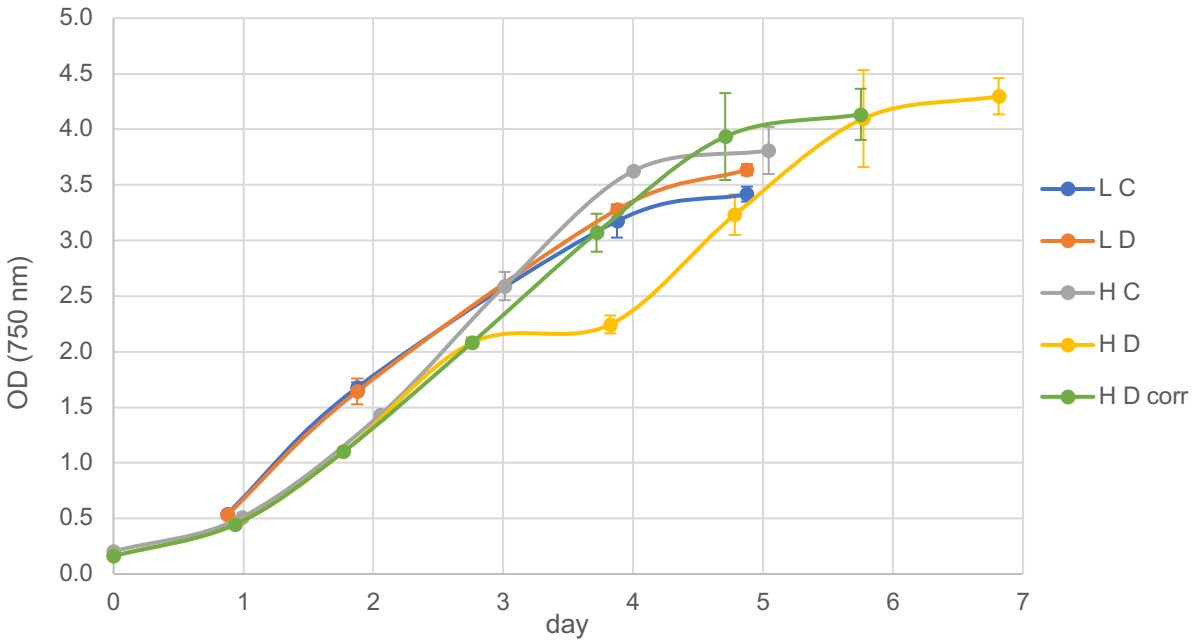

Figure 15: Optical density from the B2 strain in the Algaebator. Some samples were subjected to a higher (H) maximum light intensity (636 µE), whilst the others were under lower (L) light (318 µE). For each scenario there were four Erlenmeyer flasks with (D) and two without (C) dodecane. The corrected curve for the samples under high light and with a dodecane layer (H D corr), where the effect of the day without CO_2 was removed, is also displayed. Day zero is the day of the inoculation.

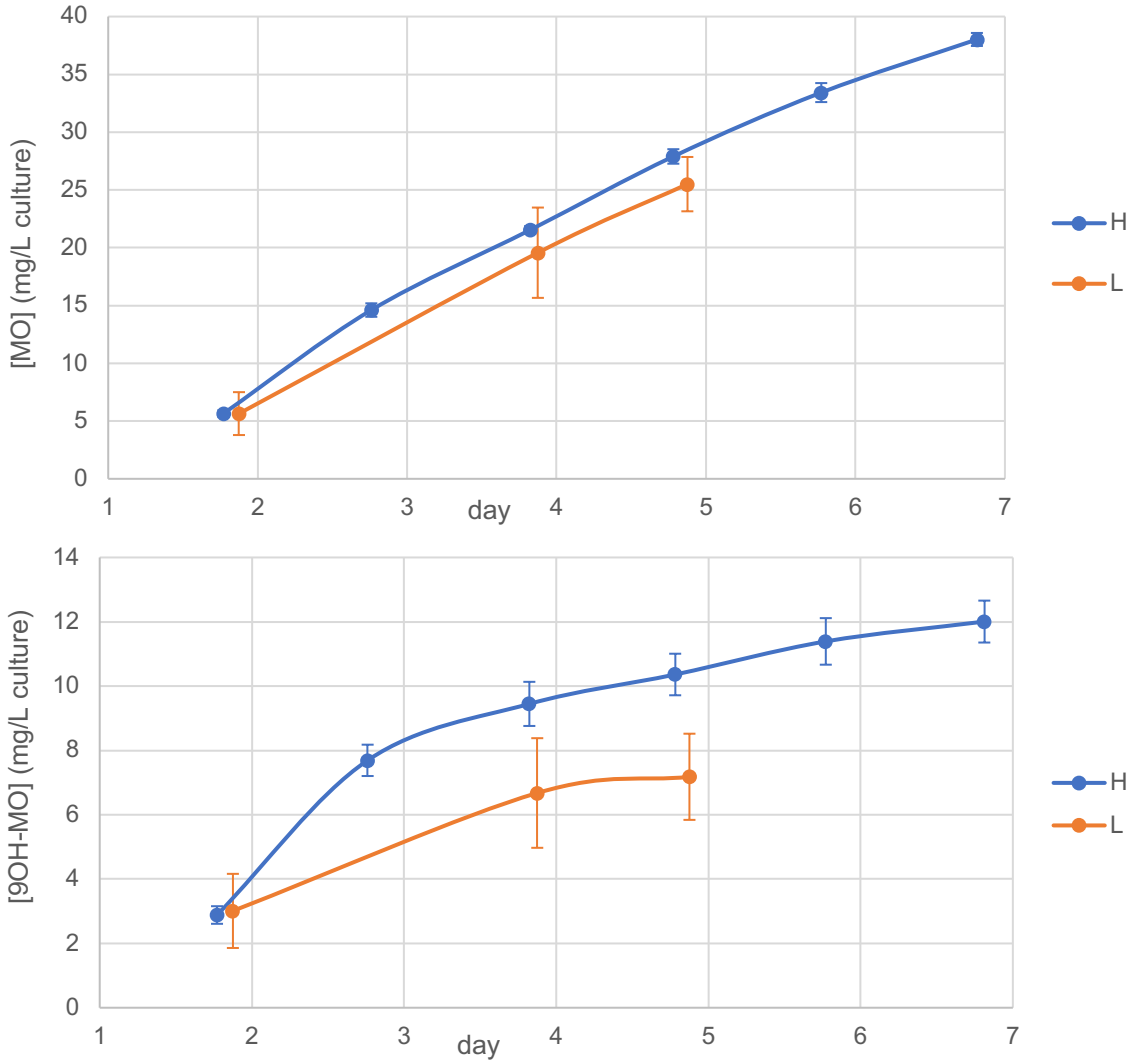

Figure 16: Manoyl Oxide (top) and 9-hydroxy-Manoyl Oxide (bottom) concentration in mg per L of culture. Some samples were subjected to a higher (H) maximum light intensity (636 µE), whilst the others were under lower (L) light (318 µE). Day zero is the day of the inoculation, the dodecane was introduced in the Erlenmeyers at day one.

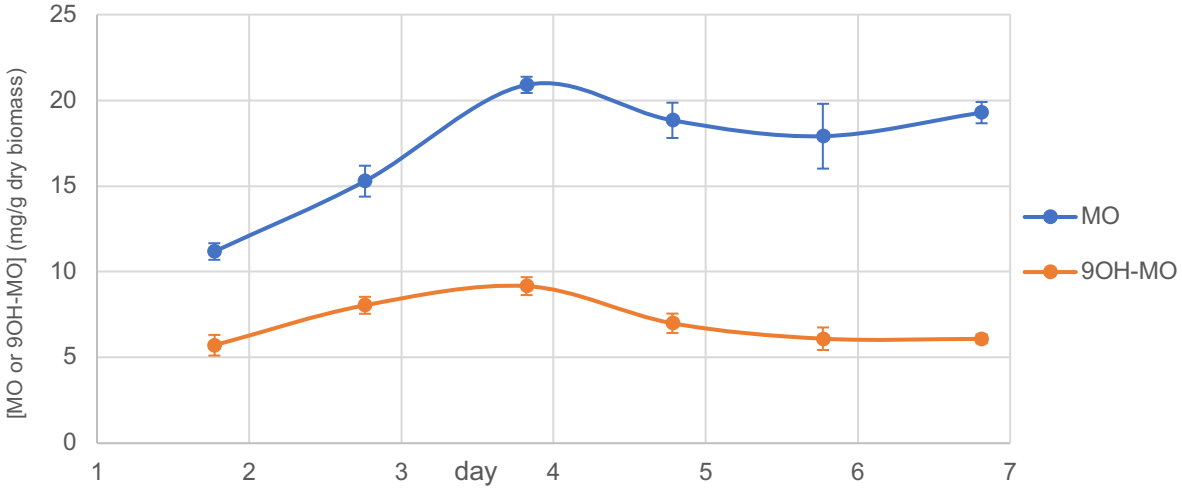

Figure 17 - Manoyl Oxide and 9-hydroxy-Manoyl Oxide concentration in mg per mass of dry biomass. All samples were subjected to 636 µE. Day zero is the day of the inoculation, the dodecane was introduced in the Erlenmeyers at day one.

4.1.3. Productivities Comparison

The productivities for the two experiments are summarized in the following table.

Table 1: Biomass, Manoyl Oxide and 9-hydroxy-Manoyl Oxide productivities from both experiments in the algaebator. First from both strains with 318 µE (L) of light intensity, then B2 strain at 636 µE (H).

	Biomass·10[1] ($gL^{-1}day^{-1}$)	**MO ($mgL^{-1}day^{-1}$)**	**MO ($mgg^{-1}day^{-1}$)**
B1 L	3.9±1.4	7.5±1.5	6.7±4.6
B2 L	3.8±1.3	6.2±0.7	5.2±2.0
B2 H	3.7±1.5	6.3±1.5	3.2±4.7
	Biomass·10[1] ($gL^{-1}day^{-1}$)	**9OH-MO ($mgL^{-1}day^{-1}$)**	**9OH-MO ($mgg^{-1}day^{-1}$)**
B2 L	3.8±1.3	1.8±1.3	1.8±1.9
B2 H	3.7±1.5	2.0±1.5	1.0±2.7

The obtained productivities were lower than the ones recorded by Lauersen *et al.* (2018), who extracted between 30 and 50 mg/L of Manoyl Oxide in 7 days, being that the maximum corresponds to 81.3 mg/g. That is around 11.6 $mg \cdot g^{-1}day^{-1}$, twice of what was achieved during these experiments. Considering that higher light intensities were used, and that there was a higher contact area per volume in this set-up, such results were unexpected. This could be related to an erroneous quantitative analysis, and it will be further discussed in section 4.5. The lower terpenoid's productivity per mass of dry biomass is probably due to the impact of CO_2 privation and restoration in the cells.

To conclude, these two experiments allowed us to compare both strains and gather more data on their performance under more realistic conditions. Biomass and Manoyl Oxide productivities were similar between different strains and light intensities. Using TAP Medium, they've reached a biomass concentration around 1.7 g/L and showed no light sensitivity at 636 µE. Although B2 strain produces 9-hydroxy-Manoyl Oxide, it still produces around three times more Manoyl Oxide.

In the last experiment, samples to assess the MO concentration in both the medium and inside the cells were also taken, which will be further explained in section 4.4.

4.2. Reactor Process Design

During this thesis, a big emphasis was given to the transition from Erlenmeyers to flat panel photobioreactors, the first step of a future scale up. In the beginning, 400 mL bioreactors named *Algaemists* were used to grow the microalgae, which would temporary leave the reactor to enter the extraction vessel containing a layer of dodecane, to then return to the reactor by the means of an auxiliary pump. Some changes had to be made from the first design to the one used in the experiment, mainly to increase the flow inside the tubes carrying the algae in and out the extraction vessel. Initially the liquid had a flow rate of 5.56×10^{-8} $m^3 s^{-1}$, which corresponded to a speed of 4.42×10^{-3} ms^{-1} and a Reynolds number of 17.7. At such a low speed, the biomass was depositing inside the tubes at a rate higher than expected due to the reduced mobility from these strains, a consequence from having no flagella, compromising the whole process. In order to solve this problem, thinner tubing was used, as well as two pumps in parallel for each way. This increased the flow rate to 2.55×10^{-7} $m^3 s^{-1}$, the speed to 0.144 ms^{-1} and Reynolds to 216.

Further investigation led to the conclusion that the speed of the fluid inside the tubes should be higher than 2×10^{-2} ms^{-1} and transitions in tubbing diameter should be avoided, since that creates sudden increases in pressure which foment the biomass deposition. Nevertheless, the conditions previously described with a speed of 0.144 ms^{-1} were used, given that it was the maximum achievable with the built set up and that it was in our interest to have the content of the reactor and the extraction vessel as similar as possible, so that the overall mixture could be considered as uniform. The reason for this requirement will be further explained in section 4.4.

Initially, the biomass grew inside the reactor in batch mode, until an OD around 1.3 was reached. After that the reactor was kept in turbidostat, guaranteeing the concentration would remain constant, until the system reached a steady state. Then the turbidostat mode was turned off, allowing the biomass concentration to increase to an OD around 2.8, at which it was turned on again. This time, the concentration wasn't kept as constant as before, as we can see in the following graph.

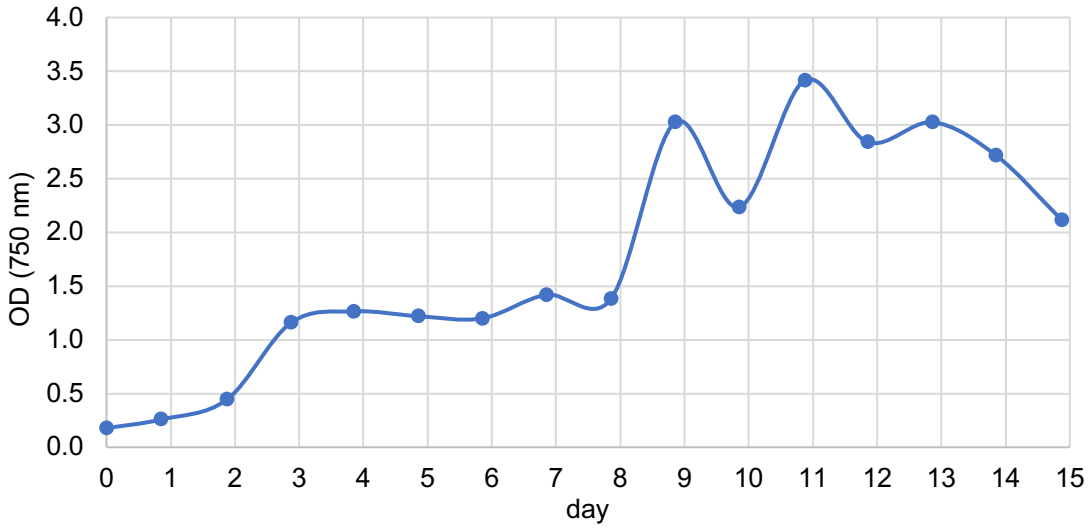

Figure 18: Optical density from daily samples from the Algaemist. Day zero is the day of the inoculation. The turbidostat pump was on from day 3 to day 8 with an OD of 1.3±0.1, which corresponds to 0.59 g/L, and again with an OD of 2.8±0.5, or 1.3 g/L, from day 9 until the end of the reactor run.

The first drop in the OD from day 9 to day 10 was due to a miscalculation when defining the outgoing light set point, which was corrected the following day. Somewhere during the night of day 11 or dawn of day 12, the magnetic stirrer inside the extraction vessel stopped working, provoking the deposition of biomass inside the bottle and the second drop in OD observable in the graph. On the last two days of the experiment the liquid level inside the extraction vessel and the reactor became unstable, as the pump tuning became more difficult. This was probably due to the state of the pump tubing material, which was slightly distended after non-stop work for over a week, and some eventual contact with dodecane drops which managed to escape the bottle. This hypothesis was supported by a slight swelling of the silicone tube inside the overflow vessel, an indicator of dodecane contact. However, the amount of dodecane which might have escaped was too small to be noticed or significantly vary the volume of dodecane layer, and it would escape the reactor fast enough not to disturb neither the growth of the microalgae nor the extraction system.

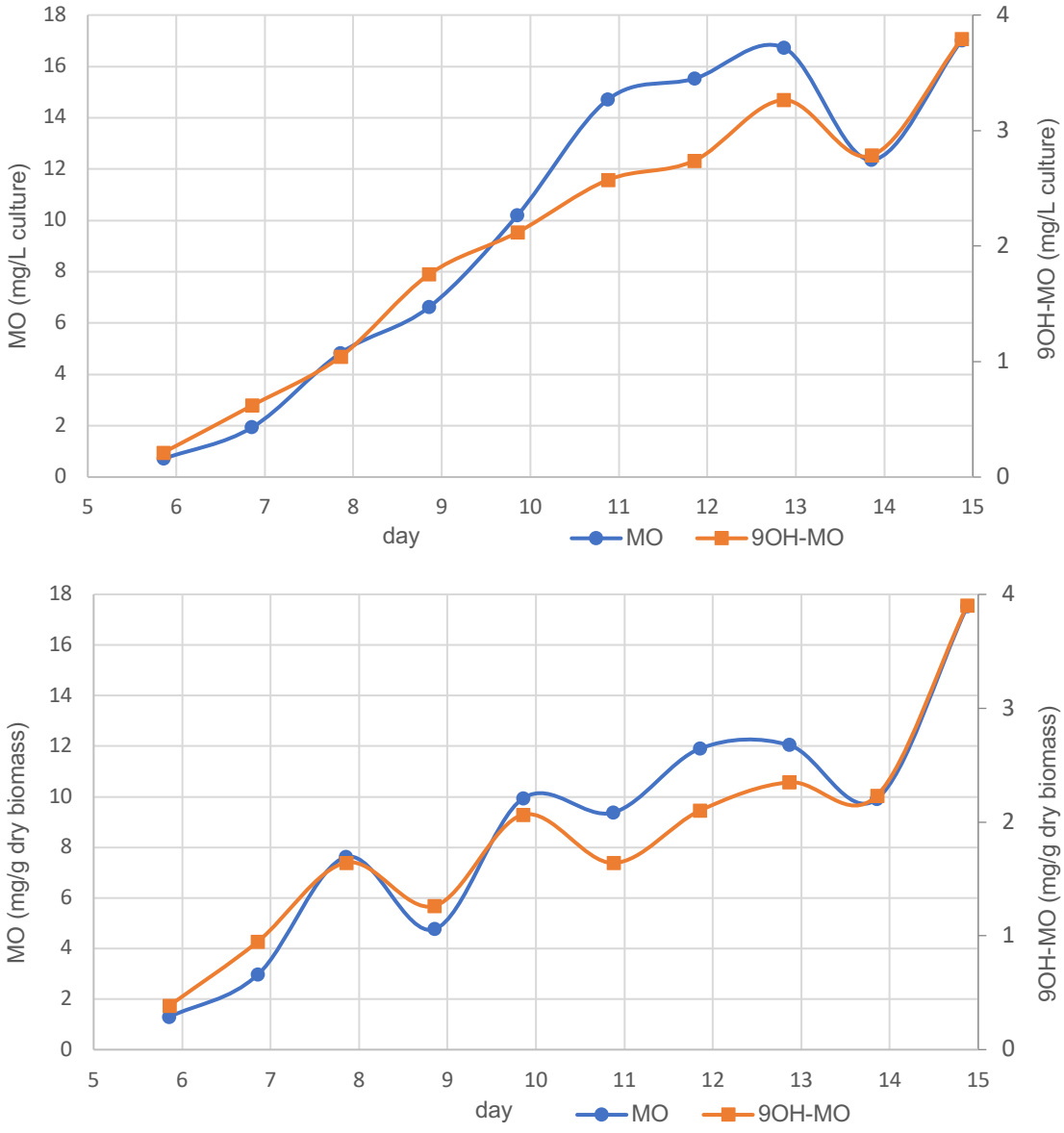

Figure 19: Manoyl Oxide and 9-hydroxy-Manoyl Oxide extracted by the dodecane layer in contact with the culture from the Algaemist, in mg per L of culture (top) and in mg per mass of dry biomass (bottom).

The Manoyl Oxide extraction rate appears to decrease after the magnetic stirrer incident, but this is mainly caused by the decrease in biomass concentration, as can be seen when plotting the MO concentration per mass of microalgae (Figure 19). Given that the terpenoids were getting accumulated in the dodecane, their concentration could never decrease. That being said, the strange drop on day 14 has no physical meaning, most likely caused by the creation of MO gradients throughout the dodecane layer due to the formation of emulsion.

It should be noticed that the drop from day 8 to day 9 in the bottom graph from Figure 19 corresponds to the time the reactor was in batch mode again and that the biomass concentration increased significantly in a short span of time. Even though MO was still being produced and extracted and the biomass growing at the same rate as before, the sudden increase on its density leads to the observed drop. The same situation happened from day 10 to day 11.

Table 2: Manoyl Oxide and 9-hydroxy-Manoyl Oxide average productivities for the culture in the Algaemist.

MO (mg/Lday)	**MO (mg/gday)**	**MO (mg/mol$_{light}$)**
1.7±2.6	1.8±2.4	1.8±2.8
9OH-MO (mg/Lday)	**9OH-MO (mg/gday)**	**9OH-MO (mg/mol$_{light}$)**
$(3.8\pm3.9)\cdot10^{-1}$	$(4.0\pm3.7)\cdot10^{-1}$	$(4.1\pm4.1)\cdot10^{-1}$

By comparing the values from the above table with the productivities calculated for the Erlenmeyers experiments, we observe that the terpenoids' productivities are significantly smaller in the reactor than in the Erlenmeyers. A reason for this could be the difference in contact time between the cells and the solvent. In the Erlenmeyer flaks, biomass is constantly in contact with the dodecane, while inside the reactor, it stays in contact with the solvent layer only during 10 minutes for every 40 minutes. Another important factor is the mass transfer area to volume ratio, which is higher for the Erlenmeyers than for the *Algaemist*.

4.3. Scaling-up at Lab-scale

The next step was to create the same set up with a bigger reactor. A 2L flat panel photobioreactor named *Infor* was used. Consequently, a bigger extraction vessel was used, but still the ratio between volume of dodecane and culture was reduced to half. Both reactors were run in batch mode until reaching the desired biomass concentrations, at an OD of 4 and 6 for *Infors* A and B respectively. They were then operating in turbidostat from day 7 onwards, however the concentrations didn't remain as constant during this period as expected, showing a 27% and 13% deviation from the average concentration on reactor A and B, respectively (Figure 20).

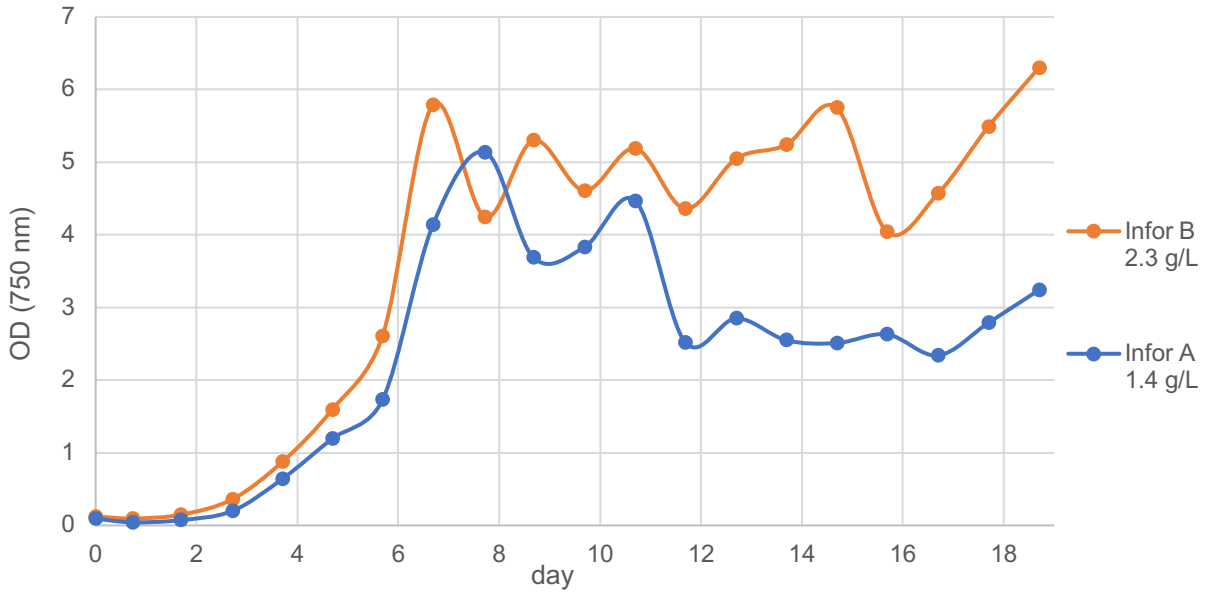

Figure 20: Optical density from daily samples of both Infor reactors on the first run. Day zero is the day of the inoculation. The turbidostat pump was on from day 7 to day 19, with an OD of 3.0±0.7 for Infor A, which corresponds to a biomass concentration of 1.4 g/L, and an OD of 5.1±0.7 for Infor B, which corresponds to 2.3 g/L.

At such biomass concentrations and a light intensity of 636 µE, the outgoing light was too low to allow a proper control based on this value. More specifically, at the moment the turbidostat was turned on the outgoing light value was around 2 µE in both reactors, despite the different OD's. This allowed the concentration inside the reactors to vary during the first couple of days in turbidostat.

From day 11 to day 12 there was a drop in both reactors' curves due to an extraordinary medium addition. The liquid level inside the reactors had decreased and the dilution rate was very low, which led me to compromise the stability of the microalgae concentration for the sake of having a healthy growing culture, by manually adding fresh medium to the reactor until the liquid level was back to normal. This had a bigger influence in reactor A, since its dilution rate increased significantly after this event, as we can see in the graph plotted below (Figure 21). In fact, this situation was repeated for reactor B, causing the drop from day 15 to day 16. At this point, the computer where the controlling sequence was written was frozen, which didn't damage the run but also didn't allow us to change the outgoing light set point. For this reason, from day 16 onwards Infor B was almost running in batch, which can also be noticed in the curve's flattening in the next graph.

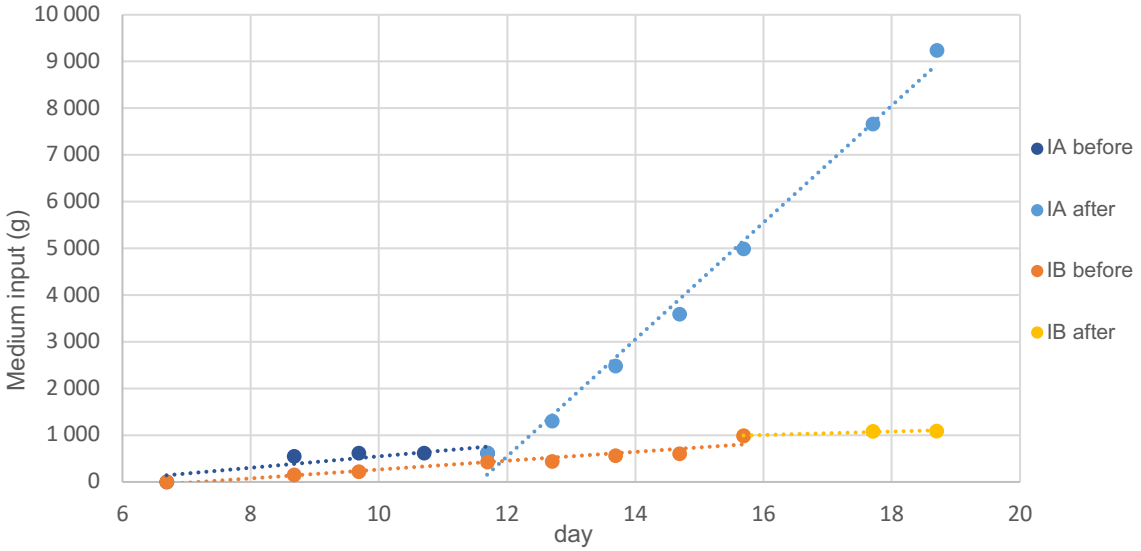

Figure 21: Medium added to the reactor accumulated over time, starting on the first day the turbidostat was on. The curves are split in before and after the manual medium addition that had the biggest impact on the reactor.

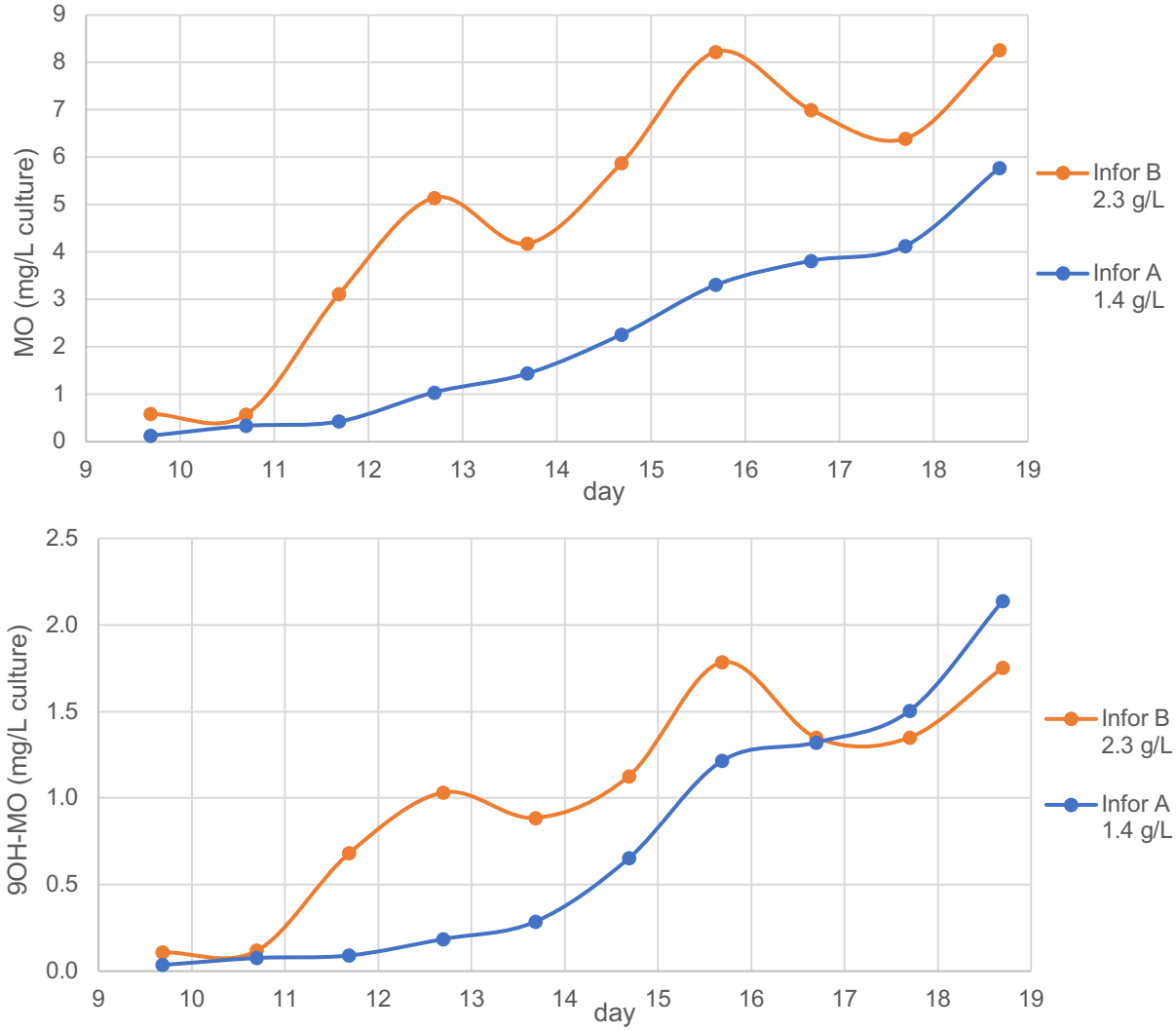

Figure 22: Manoyl Oxide (top) and 9-hydroxy-Manoyl Oxide (bottom) extracted by the dodecane layer in contact with the culture from the Infors on the first run, in mg per L of culture.

Once again, the emulsion formed from the contact between the dodecane and the culture phase generated gradients throughout the solvent layer. For this reason some samples were not very representative, leading to the two drops which can be seen in the curves from reactor B in Figure 22.
After analysing the growth curves and rate, it was hypothesised that the cells might have been light limited at the highest concentrations, which was corroborated with how the dilution rate increased when the reactor was operating at lower densities. To explore this possibility, a second run was performed, once again with two reactors. Initially, they were run in luminostat instead of batch, so that the ingoing light would increase proportionally to the microalgae growth, and eventually reach a higher level than before. It so happened with *Infor* C, which ended up with the value of 2815 µE as light intensity, over four times higher than the one used so far, with an outgoing light of only 8 µE. After turning on the extraction system on day 5, the consequent dilution doubled the secondary light, and for that reason the primary one was reduced to 1877 µE and kept in this way until the end of the experiment.
The same did not happen with *Infor* D, which grew at a very slow pace in luminostat mode. For this reason, a light intensity of 636 µE was used as before, only with a much lower biomass concentration.

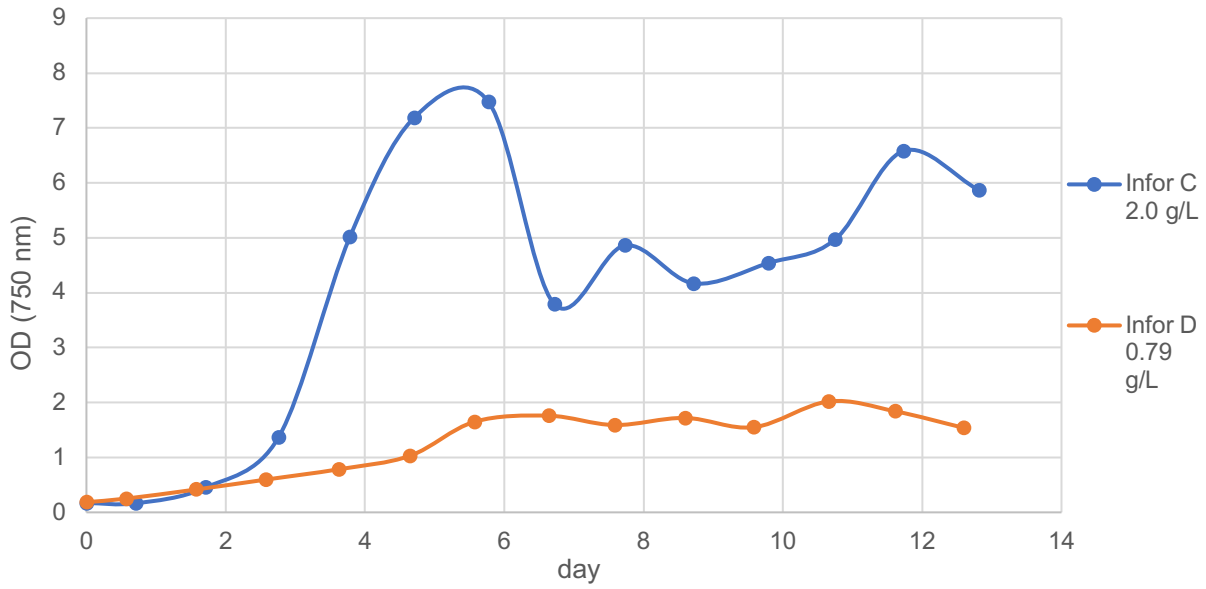

Figure 23: Optical density from daily samples of both Infor reactors on the second run. Day zero is the day of the inoculation. The turbidostat pump was on from day 6 in reactor D, with an OD of 1.7±0.2 and biomass concentration of 0.79 g/L. In reactor C, the turbidostat pump was on from day 4, but only the points from day 7 to day 10 (inclusive) were taken into consideration for further analysis, which corresponds to an OD of 4.3±0.5 and biomass concentration of 2.0 g/L.

On day 6, the turbidostat control was turned on at reactor D. From this point onwards the culture was growing steadily, looking healthy and with a quantum yield of 0.7. Overall it had an optical density of 1.7±0.2, which corresponds to a 9,6% deviation and a biomass concentration of $(7.9\pm0.9)10^{-1}$ g/L.
Reactor C was operating in turbidostat from day 4 onwards. At such high primary light and low secondary light intensities it was hard to control the biomass concentration based on the outgoing light, as noticeable variations in the culture density will lead to very small changes on the control variable. For

this reason, the concentration still increased during the first day in turbidostat. The extraction system was turned on at day 5, but sadly a mistuning of the pumps made the whole content of the extraction vessel enter the reactor. The large majority of the dodecane ended up in the overflow vessel, some in the airlock and a small leftover stayed inside the reactor. The efforts for this leftover to go to the overflow included turning on the feed pump, which caused the drop in OD visible from day 6 to day 7. A fresh layer of dodecane was introduced in the bottle and the extraction system was restarted on day 6, only for the same situation to repeat itself on day 11. This time, the dodecane leftover inside the reactor remained inside until the end of the experiment. After the first incident, direct observation indicated that the culture wasn't as healthy as before, since it now had a more yellowish shade of green and had started to foam. A quantum yield between 0.5 and 0.6 and an abrupt decrease in the dilution rate (Figure 24) support these observations. Due to the described incidents, only the data points from day 7 to 10, inclusive, were taken into consideration for further analysis.

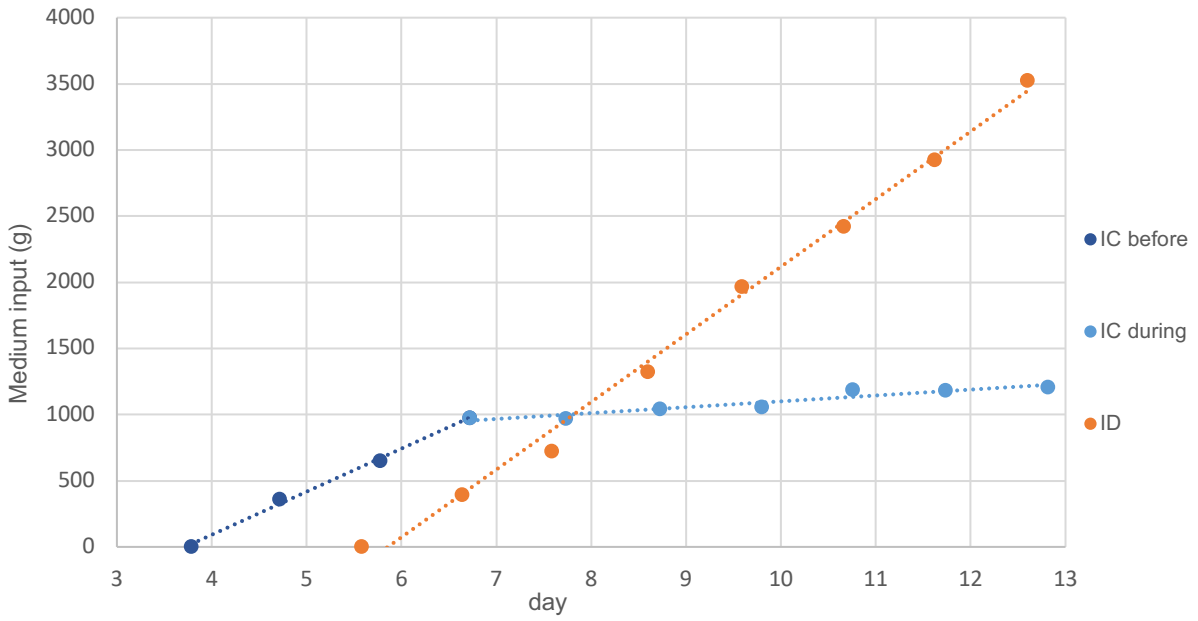

Figure 24: Medium added to the reactor accumulated over time, starting on the first day the turbidostat was on. The curve from Infor C is split at the point when its dilution rate significantly changed.

With this in mind, it seems intriguing the way the optical density increases from day 11 to day 12, right after the second incident. However, the ratio between the optical densities at 680 and 750 nm decreased from 1.17 to 1.12 at this point, along with the quantum yield. That being said, the microalgae growth might not have been the main driver of the observed increase in turbidity.

Similarly to what happened in the first run, the reactor with the lowest dilution rate, Infor C, was the one where bigger MO titters were obtained, as can be seen in Figure 25. The several biomass concentrations and MO productivities from each run are summarized in the Table 3.

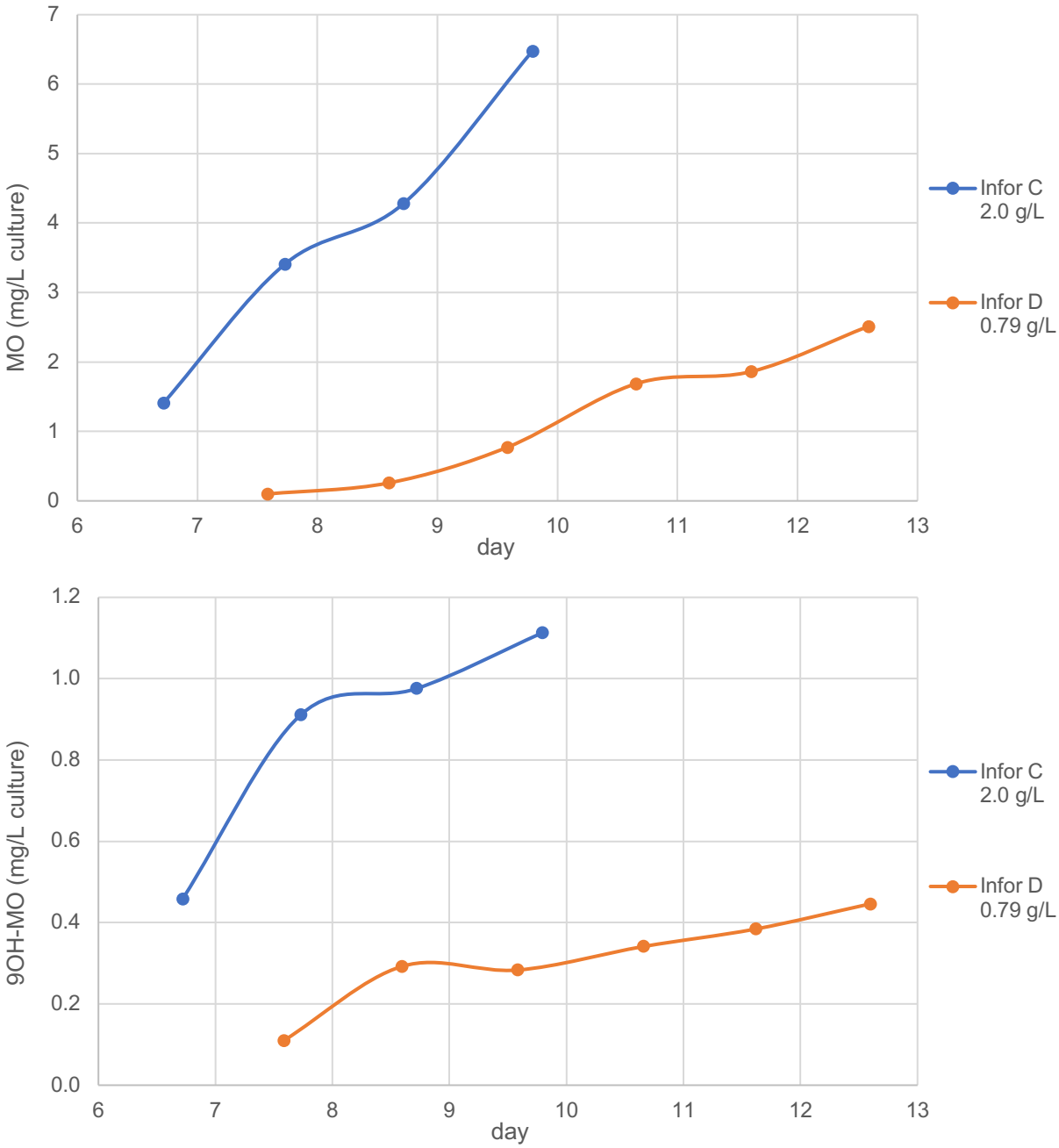

Figure 25: Manoyl Oxide (top) and 9-hydroxy-Manoyl Oxide (bottom) extracted by the dodecane layer in contact with the culture from the Infors on the second run, in mg per L of culture.

From comparing the three runs at 636 µE (Table 3), we can observe that the extracted Manoyl Oxide per biomass decreases with the increase in biomass concentration, while the productivities per volume of culture and light both increases, as expected. Looking at reactors B and C, which have a considerably similar biomass concentration, we can see that the biomass productivities are double at the highest light intensity, while the light productivity is understandably lower. Different trends can be seen for the 9-hydroxy-Manoyl Oxide. Amongst the three reactors at 636 µE, the reactor A is the one where a higher productivity was achieved, indicating this reactor offered the most optimal conditions for this terpenoid

to be formed. Once again, reactor C had higher productivities per volume of culture and per mass of biomass than reactor B, and lower light productivity.

Table 3: Optical densities (OD), biomass concentration (x), Manoyl Oxide (MO) and 9-hydroxy-Manoyl Oxide (9OH-MO) productivities and primary light intensities for the four studied scenarios.

Infor	**OD (750 nm)**	**x (g/L)**	**MO·10^1 (mgL^{-1}day^{-1})**	**MO·10^1 (mgg^{-1}day^{-1})**	**MO·10^1 (mg/mol$_{light}$)**	**Light (µE)**
A	3.0±0.7	1.4±0.3	5.8±4.8	4.5±3.6	2.1±1.8	636
B	5.1±0.7	2.3±0.3	8.3±14.5	3.7±6.7	3.0±5.3	636
C	4.3±0.5	2.0±0.2	15.5±6.5	7.6±2.6	1.9±0.8	1877
D	1.7±0.2	0.79±0.09	4.2±3.3	5.3±3.9	1.5±1.2	636
Infor	**OD (750 nm)**	**Biomass (gL^{-1}day^{-1})**	**9OH-MO·10^2 (mgL^{-1}day^{-1})**	**9OH-MO·10^2 (mgg^{-1}day^{-1})**	**9OH-MO·10^2 (mg/mol$_{light}$)**	**Light (µE)**
A	3.0±0.7	0.86	21±23	17±17	7.8±8.3	636
B	5.1±0.7	0.11	18±33	8±16	6±12	636
C	4.3±0.5	0.044	26±18	13±11	3.4±2.6	1877
D	1.7±0.2	0.20	7.4±6.5	9.5±8.5	2.7±2.4	636

All productivities are considerably lower than the ones registered in the *Algaemist* experiment (Table 2 and Table 3). Once again, the main reasons for this are a lower area to volume ratio and a smaller proportion between the time spent in contact with the extraction solvent and the time spent inside the reactor. More specifically, the mass transfer area per volume of culture was around 2.5 times smaller than before, and the cells would remain for 13 minutes inside the extraction vessel for every two hours spent in the growth chamber. In fact, if the MO productivity per mass of culture from the experiment in the *Algaemist* is used to estimate the productivity in the *Infor* reactors, taking only these two parameters into consideration and assuming a linear proportionality between them and the productivity, the value $3.1 \cdot 10^{-1}$ mgg^{-1}day^{-1} is obtained, which is in line with the results from Table 3. One must bear in mind that this is a rough estimation, as factors such as the light intensity and light path also play an important role. Furthermore, in this last *Infors* experiment, the cells viability was assessed both right before the extraction system was turned on and at the end of the experiment, in order to evaluate its effect on the cells. The percentage of non-viable cells increased from 2-4% to 7-9% during the time the cells where submitted to the pump and contact with dodecane. These values are lower than the ones registered for *Dunaliella Salina* in contact with a dodecane overlayer, where a cell death rate of around 20% was observed after four days (Kleinegris 2010).

4.4. Manoyl Oxide production and transfer mechanism

4.4.1. Steady state

This section is dedicated to the understanding of the production, excretion from the cells and transfer from aqueous to organic phase mechanisms. This study was made based on the model created by Heinrich *et al.* (to be published), which will be explained here in a synthetic way. This model was first created assuming steady state, such as the one reached when the reactors are operating in turbidostat mode. Further on, it was adapted for a transitory state, to describe the situation from the algae growing inside the Erlenmeyers in the algaebator.

The model is based on several assumptions, which will be shortly explained and, when needed, verified:

1. Biomass, CO_2, Oxygen, light and other nutrients are in steady state, which can be achieved by using turbidostat control.
2. Biomass growth and Manoyl Oxide production are considered independent reactions.
3. The Manoyl Oxide is actively exported from the inside of the cells to the reactor medium.
4. Biomass death is not taken into account. Considering that the percentage of non-viable cells found in the system was from 7 to 9%, it is reasonable to neglect cell death's effect.
5. The dissociation of both Manoyl Oxide and its hydroxylated version were neglected at the working pH. Considering that the pKa from the OH group from 9-hydroxy-Manoyl Oxide is 13.36 (Chemicalize) and that the remaining protons are in more stable positions, it is quite reasonable and safe to assume this.
6. The reactor is a well-mixed continuous stirred tank reactor. This was assured inside the reactor with airflow circulation, and inside the extraction vessel with a magnetic stirrer.
7. The properties of the medium inside the reactor and the extraction vessel are the same, and the total reactor working volume is the sum of the aqueous phase in both vessels. This is assured by making the residence time of the culture inside the extraction vessel significantly lower than the residence time in the growth vessel. With the *Infor* reactors, the residence time inside the reactor was almost 2h, whilst the culture would remain only 13 minutes inside the vessel with the solvent.
8. The density of the medium entering the reactor and the medium inside it can be considered equal.
9. The volumes of dodecane and medium in the system are considered constant, neglecting losses due to evaporation and sampling.

Based on mass balances to the biomass and to the Manoyl Oxide inside the cells, in the dodecane layer and in the culture, the following differential Equation System was reached:

$$\mu = \frac{Q}{V_R} \tag{3}$$

$$\frac{dm_{MO}^{X}}{dt} = \frac{r_{MO}}{x} - \frac{r_{EX}}{x} \tag{4}$$

$$\frac{dm_{MO}^{DD}}{dt} = \frac{V_R}{V_{DD}} k_T a\left(K_4 m_{MO}^{AQ} - m_{MO}^{DD}\right) \tag{5}$$

$$\frac{dm_{MO}^{AQ}}{dt} = -\frac{Q}{V_R}\left(m_{MO}^{AQ} + x m_{MO}^{X}\right) - k_T a\left(K_4 m_{MO}^{AQ} - m_{MO}^{DD}\right) + r_{EX} \tag{6}$$

Where μ represents the specific growth rate, x the biomass concentration, m_{MO}^{X}, m_{MO}^{AQ} and m_{MO}^{DD} the Manoyl Oxide concentration in the pellet, supernatant and dodecane, respectively, r_{MO} and r_{EX} the Manoyl Oxide production and excretion rates, V_R and V_{DD} are the volume of culture and of dodecane in the system, K_4 is the equilibrium constant between the Manoyl Oxide concentration in the organic and in the phases, k_T is the mass transfer coefficient and *a* is the concentration of exchange area. K_4 was estimated using Chemicalize, having the value of $10^{5.50}$. In order to calculate the Manoyl Oxide production and excretion rates, the content of Manoyl Oxide in the pellet and supernatant were measured in addition to the measurements already mentioned. These were plotted in the graphs bellow.

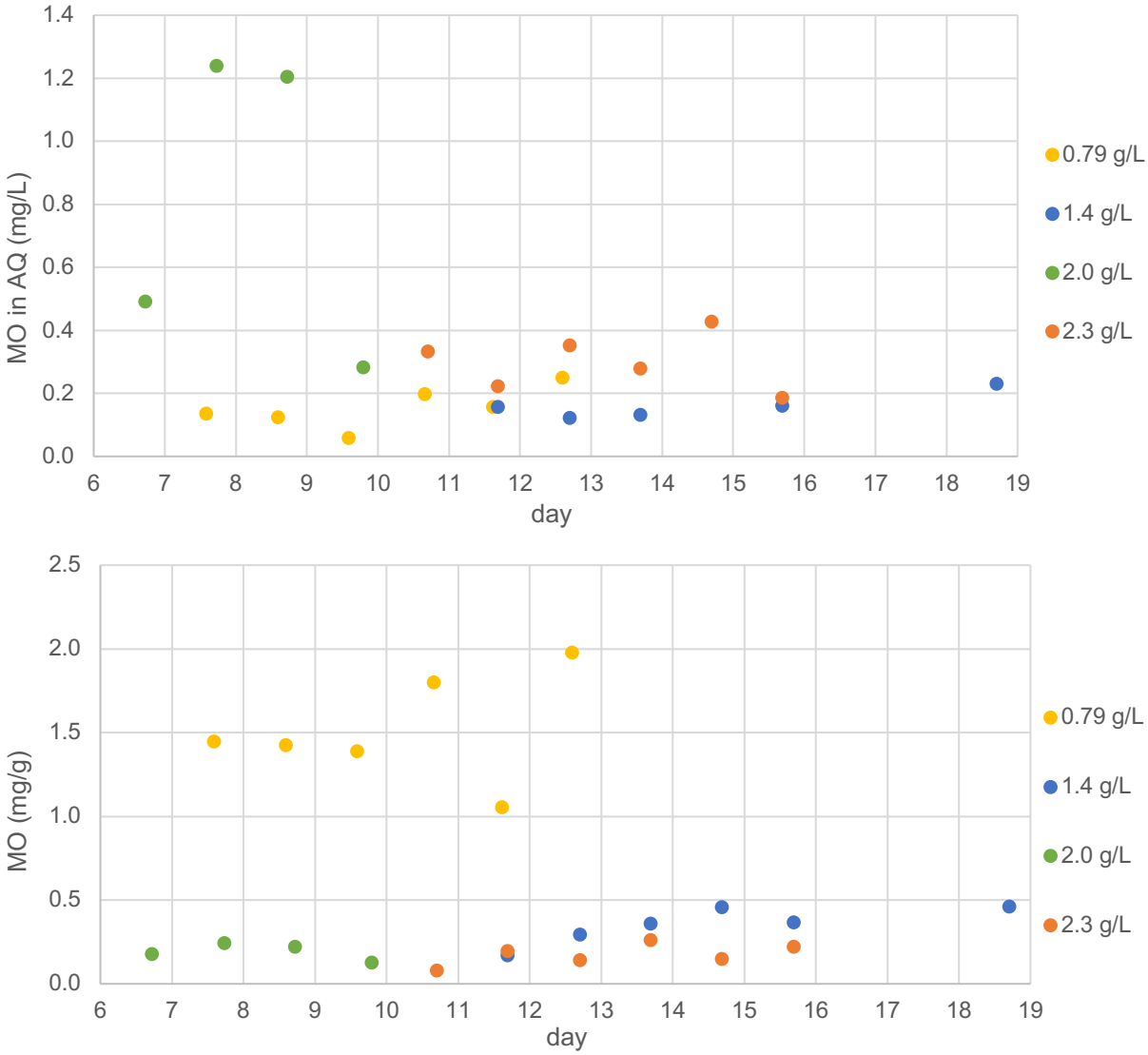

Figure 26: Manoyl Oxide concentration in the supernatant (AQ), in mg per L of culture (top), and in the pellet (X), in mg per mass of culture (bottom), in the four different Infor runs.

Looking at the three reactors with a light intensity of 636 μE during the turbidostat, which corresponds to the ones with 0.79, 1.4 and 2.3 g/L of biomass concentration, we have $(2.1\pm0.6)10^{-1}$ mg MO/L of culture in the aqueous phase. More importantly for the current analysis, we can consider this concentration to be constant over time. Looking at the concentration inside the pellet, it can also be

considered roughly constant over time. However, this time the three runs with a higher biomass concentration have more similar values, with an average of $(2.2\pm0.9)10^{-1}$ mg MO/g cells. With this in mind, the time derivatives from m_{MO}^{X} and m_{MO}^{AQ} can be considered zero and an average value for these concentrations can be used. Since m_{MO}^{DD} is significantly smaller than $K_4 m_{MO}^{AQ}$, this can be neglected and $K_4 m_{MO}^{AQ} - m_{MO}^{DD} \approx K_4 m_{MO}^{AQ}$ in both 5 and 6. In this way, we can easily calculate $k_T a$ from 5 and then use it to obtain r_{EX} from 6 and r_{MO} from 4. To be noticed that the rate of excretion is the same as the rate of production, given that the concentration of Manoyl Oxide inside the pellet is constant. On Table 4, it can be seen that the production and excretion rates are quite similar for all the four different runs, with an average value of $(1.2\pm0.3)10^{-3}$ $gL^{-1}day^{-1}$. Curiously, the $k_T a$ values from the three runs at 636 μE are also alike, with an average of $(1.3\pm0.3)10^{-5}$ day^{-1}, but it drops to half in the reactor running with 1877 μE of light intensity. There are no reasons to believe $k_T a$ should be lower in a higher light intensity scenario, and a larger collection of data should dissolve such differences. The overall average value for $k_T a$ is $(1.1\pm0.4)10^{-5}$ day^{-1}.

The 9-hydroxy-Manoyl Oxide concentration is also constant over time both in the medium and inside the cell, so all calculations were made in a similar way as for the Manoyl Oxide. To be noticed that now K_4 has the value of $10^{4.57}$ (Chemicalize). Sadly, there was no data regarding the amount of 9OH-MO in the aqueous phase from the reactor at a biomass concentration of 0.79 g/L, so this had to be estimated. Assuming that $k_T a$ would be similar amongst the three reactors at 636 μE, the average from reactors with 1.4 g/L and 2.3 g/L was used as the $k_T a$ for the lowest biomass concentration. It was assumed only these three reactors to be similar and not all of them, for that was the trend observed for these particular cases. From there, the concentration of the 9OH-MO in the aqueous phase was calculated, and all remaining parameters obtained using that value. The average values are (8.3 ± 2.8) 10^{-5} day^{-1} and $(2.4\pm1.4)10^{-4}$ $gL^{-1}day^{-1}$ for $k_T a$ and for the production and excretion rates, respectively. The mass transfer coefficient is almost one order of greatness bigger for the 9OH-MO than for the MO, since the decrease in K_4 increases $k_T a$, and the concentration of 9OH-MO in the aqueous phase is lower than for MO. The results for the four different runs are summarized in the following table.

Table 4: Values of $k_T a$, rEX and rMO for the different runs with different biomass concentrations, both for Manoyl Oxide and 9-hydroxy-Manoyl Oxide.

Infor	x (g/L)	$k_T a \cdot 10^5$ (day^{-1})		$r_{EX}=r_{MO} \cdot 10^4$ ($gL^{-1}day^{-1}$)	
		MO	9OH-MO	MO	9OH-MO
D	0.79	1.04	9.67	8.50	1.02
A	1.4	1.57	9.76	12.0	4.35
C	2.0	0.638	4.18	16.5	2.09
B	2.3	1.14	9.58	11.2	2.33

Using average concentration values and the specific growth rate, the fractions of Manoyl Oxide productivity in the pellet, supernatant and dodecane overlayer where calculated, as can be seen in the next graphs.

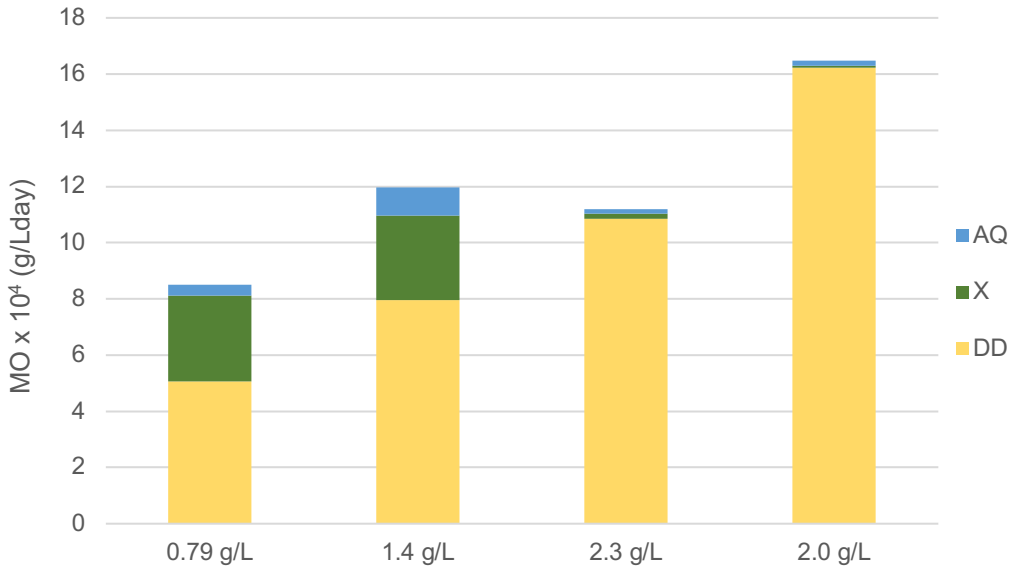

Figure 27: Manoyl Oxide productivity fractions in the dodecane layer (DD), pellet (X) and aqueous phase (AQ) in g per L of culture per day. The first three runs (0.79, 1.4 and 2.3 g/L) had a light intensity of 636 µE, while the last one (2.0 g/L) was at 1877 µE.

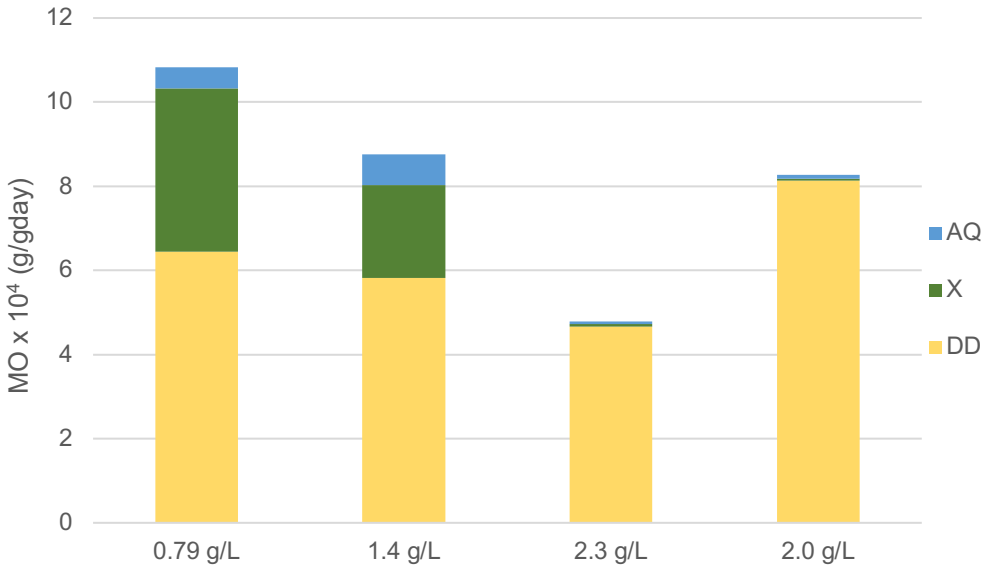

Figure 28: Manoyl Oxide productivity fractions in the dodecane layer (DD), pellet (X) and aqueous phase (AQ) in g per g of culture per day. The first three runs (0.79, 1.4 and 2.3 g/L) had a light intensity of 636 µE, while the last one (2.0 g/L) was at 1877 µE.

Looking at the three different biomass concentrations subjected to a light intensity of 636 µE in Figure 28, it is observable that the higher the biomass concentration, the less Manoyl Oxide per gram of biomass is produced. When comparing the two bars on the right side of the graph, which have a quite similar biomass concentration but different ongoing light values, the productivity in the dodecane from the reactor with 1877 µE of primary light is almost the double from the one at 636 µE. That being said, and since a lower biomass concentration leads also to a higher light per cell, this seems to be an important parameter for the production of Manoyl Oxide. Further on, we can see two different paths

towards increasing this parameter, keeping a lower biomass concentration or a higher primary light. From Figure 27 we get an indication to go through the second one, given that volume is an actual limitative logistical constrain to bear in mind. One must also consider the available sun irradiance from the place where the scaled-up project would be, in another words, if the natural conditions of the location allow for such a choice.

Our hypothesis was that the concentration of Manoyl Oxide in the aqueous phase would affect the efficiency of the process in two opposite ways. Due to an inhibition effect, an increase in concentration would decrease the production efficiency. On the other hand, it would promote the mass transfer from the aqueous to the organic phase, increasing the extraction efficiency. To assess this, the fractions of Manoyl Oxide productivity in the dodecane and in the pellet were plotted alongside the Manoyl Oxide concentration in the aqueous phase.

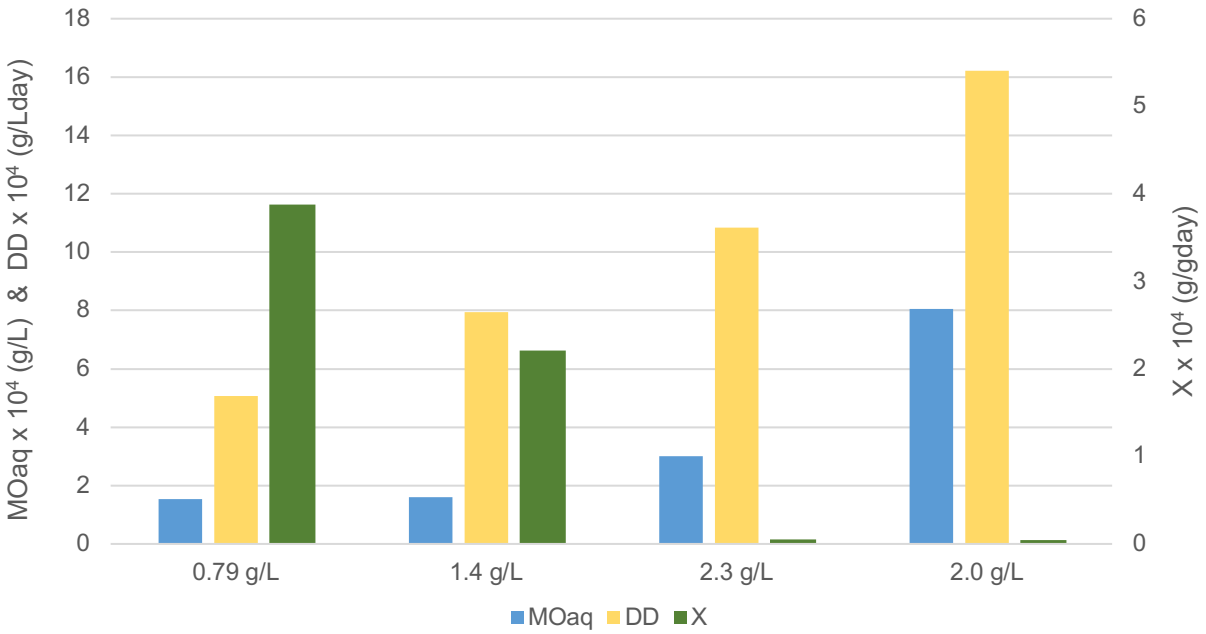

Figure 29: Manoyl Oxide concentration in the aqueous phase in g/L (MOaq) and Manoyl Oxide productivity fractions in the dodecane (DD), in g per L of culture per day, and in the pellet (X), in g per g of culture per day. The first three runs (0.79, 1.4 and 2.3 g/L) had a light intensity of 636 µE, while the last one (2.0 g/L) was at 1877 µE.

The experimental data indicate that more Manoyl Oxide is extracted with the increase in Manoyl Oxide concentration in the aqueous phase, whilst the Manoyl Oxide inside the pellet decreases with that same concentration (Figure 29). This corroborates the mentioned hypothesis and indicates not only that the mass transfer of the terpenoid from the cell to the organic solvent occurs through the aqueous phase, but also that the terpenoid concentration in the medium is a key parameter for the efficiency of the process. This is, however, a parameter harder to tune than the ingoing light, given its contradictory effects in the system. Nevertheless, a higher Manoyl Oxide concentration in the aqueous phase, and therefore a higher biomass concentration, seems to be a better option given that the amount of product which we get matters more than the one we are able to produce but not to recover.

The trend is however significantly different if the same analysis is made looking at the 9-hydroxy-Manoyl Oxide. For this terpenoid, an ideal range of biomass concentration for the tested conditions seems to have been found, as not only the total productivity but also all its fractions (in the aqueous phase, in the pellet and in the dodecane) show a maximum value for the reactor with 1.4 g/L of biomass.

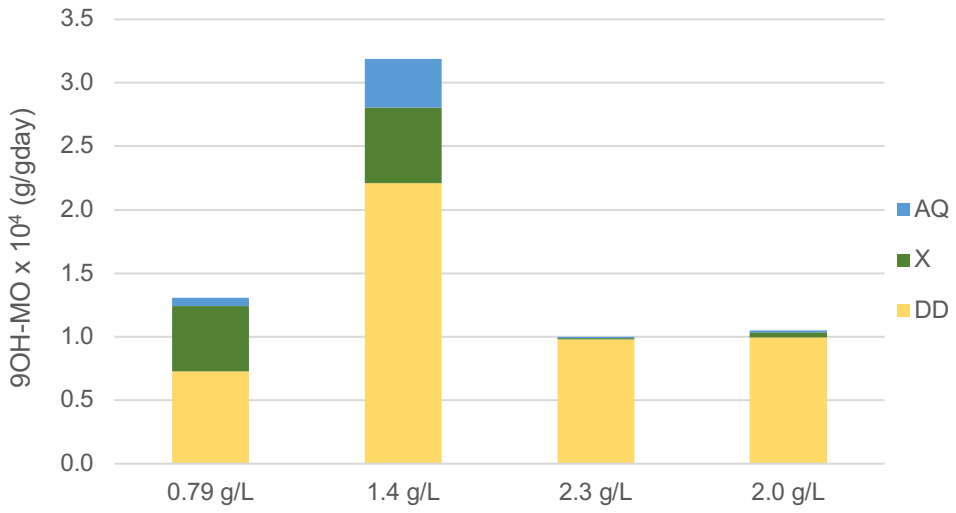

Figure 30: 9-hydroxyl-Manoyl Oxide productivities in the dodecane layer (DD), pellet (X) and aqueous phase (AQ) in g per g of culture per day. The first three runs (0.79, 1.4 and 2.3 g/L) had a light intensity of 636 µE, while the last one (2.0 g/L) was at 1877 µE.

There is no clear relation between the productivities' fractions and the terpenoid concentration in the medium. Regarding the fraction of productivity in the pellet, this indicates the presence of 9OH-MO in the medium does not inhibit the cell from converting more MO into its functionalized version. The lack of relation between the amount of 9OH-MO extracted with the dodecane and its concentration in the medium is, however, far more intriguing. When looking only at the reactors operating at 636 µE, it can still be seen that the more 9OH-MO present in the medium, the more it is extracted, as expected. However, the reactor at 1877 µE exhibits the highest product concentration in the medium and the second lowest productivity fraction in the dodecane. This seems to indicate an eventual saturation from the dodecane or an increase in affinity from 9OH-MO to the aqueous phase, or even a combination of both phenomena. Both MO and 9OH-MO have higher solubility in dodecane than the concentrations present in this particular case – in the course of this thesis, much higher concentrations from both compounds in dodecane were observed. Nevertheless, microalgae produce other terpenoids which are also extracted by the dodecane overlayer if released to the medium, thus influencing the solubility of the desired products in the solvent, such as carotenoids. Carotenoids have an important role in light harvesting and dissipation of excess light energy, and its production increases when the cells are under photooxidation stress (Guedes *et al.* 2011). Although the solubility of 9OH-MO in water is considerably low, it is significantly higher than the one from MO and ß-carotene (Chemicalize), which would explain why 9OH-MO is the compound that does not thrive in being extracted when competing with the other two. This hypothesis is weakly grounded, as there is no substantial evidence from having such high concentration of ß-carotene in the extraction solvent from this reactor. Regarding the second suggestion,

there are no reasons to believe the affinity of 9OH-MO to the aqueous phase was higher under this experiment's conditions. On the other hand, we must remember how the extraction vessel's content accidently went to the inside of this reactor right at the beginning of the experiment. Even though the majority of the dodecane exited the reactor during the next 24h and that no dodecane overlayer was visible anymore, it is possible that a dodecane leftover was still present, compromising the terpenoid accumulation in the extraction vessel. The consequence of this accident is more visible when analysing the 9-hydroxy-Manoyl Oxide than when looking at the Manoyl Oxide because lower values are being dealt with. Finally, this could also be the result of an error in the GC-FID analysis, given that this quantitative analysis tends to be less exact for smaller concentrations.

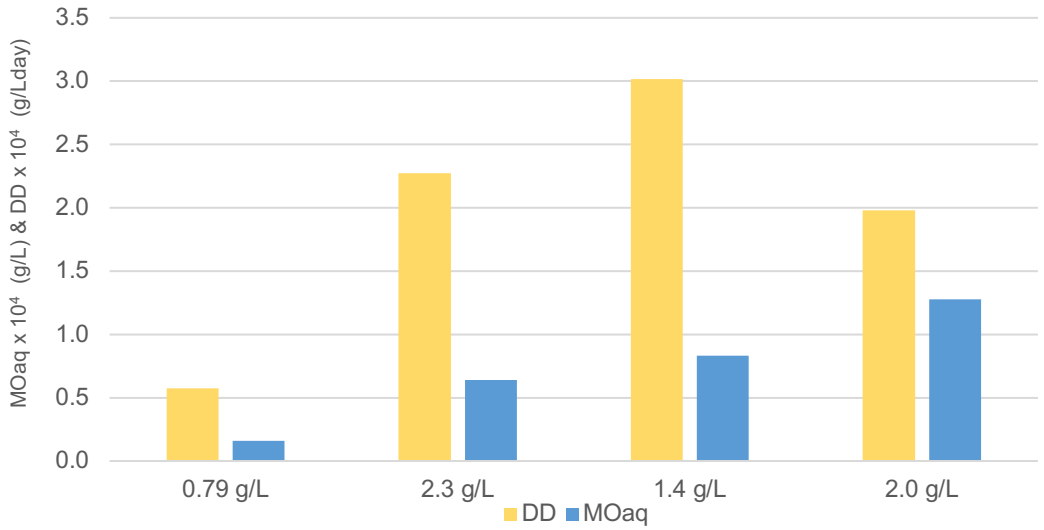

Figure 31: 9-hydroxy-Manoyl Oxide productivity fraction in the dodecane in g per L of culture per day (DD) and Manoyl Oxide concentration in the aqueous phase in g/L ([MO]aq). The first three runs (0.79, 2.3 and 1.4 g/L) had a light intensity of 636 µE, while the last one (2.0 g/L) was at 1877 µE.

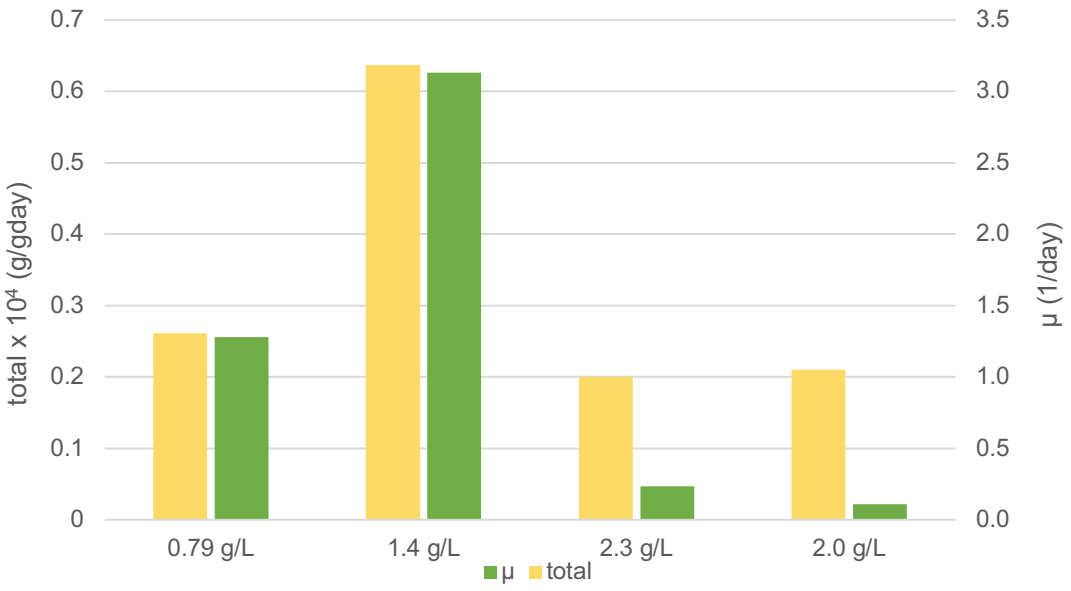

Figure 32: 9-hydroxy-Manoyl Oxide total productivity per mass of culture and specific growth rate (µ). The first three runs (0.79, 2.3 and 1.4 g/L) had a light intensity of 636 µE, while the last one (2.0 g/L) was at 1877 µE.

When plotting the total 9OH-MO productivity alongside with the specific growth rate (Figure 32), it can be seen that both these variables evolve in the same way. This highlights the close link between growth and terpenoid production from the cells, and how optimizing the conditions for one will probably optimize them for the other as well. If one would assure a higher growth rate even at higher biomass concentrations, by, for example, supplying a richer medium to the cells, the Manoyl Oxide production would probably increase. Given that the medium had twice the nitrogen and phosphate concentrations than the original recipe, which should allow the microalgae to grow to higher optical densities than the ones observed, the trace elements influence should be further analysed and eventually increased in order not to limit the cells growth at higher biomass concentrations. On the other hand, a higher dilution rate implies a higher loss of product with the overflow. This is however, directly connected to the used set up, and a concern which would not exist in different and scaled up reactor designs.

To conclude, in order to enhance Manoyl Oxide and 9-hydroxy-Manoyl Oxide production and excretion from the B2 strain and their transfer to the extraction solvent, one must optimize the growing conditions for this strain and improve the extraction system design by increasing the mass transfer area per volume ratio and avoiding the loss of product with discarded culture.

4.4.2. Transitory state

As in the previous section, the model by Heinrich *et al.* (to be published) was used to better understand the system in study, this time applied to the second experiment in the algaebator, where the system was in transitory state. All previous assumptions are still valid, apart from the first one. There are two main differences to take into consideration: first there is biomass growth, second there is no medium input nor overflow. For these reasons, 3 and Equation 6 from the differential equation system where substituted by 7 and 8, respectively.

$$\frac{dx}{dt} = r_x \qquad 7$$

$$\frac{dm_{MO}^{AQ}}{dt} = -k_T a\left(K_4 m_{MO}^{AQ} - m_{MO}^{DD}\right) - m_{MO}^{X} r_x + r_{EX} \qquad 8$$

Once again, the Manoyl Oxide content in the aqueous phase and pellet where plotted, and once again those concentrations remained roughly constant over time. The k_Ta was calculated through equation 5, and then used to calculate the production rate, obtaining the values of $(4.9\pm1.0)\cdot10^{-5}$ day^{-1} and $(6.6\pm0.1)\cdot10^{-3}$ $gL^{-1}day^{-1}$, respectively. Regarding the 9-hydroxy-Manoyl Oxide, a k_Ta of $(3.7\pm1.2)\cdot10^{-4}$ day^{-1} and a production rate of $(1.7\pm0.1)\cdot10^{-3}$ $gL^{-1}day^{-1}$ were obtained. Once again, the mass transfer coefficient was higher for 9OH-MO than for MO. The proportion between the produced MO and 9OH-MO sustains what was previously observed. The production rate is around 6 times higher in the *Algaebator* than in *Infor* reactors, which is consistent with the previous results, due to a more efficient and constantly on-going extraction.

4.5. Quantitative Analysis

In order to validate the used GC-FID method, some samples were sent to the University of Bielefeld, where they were analysed on the Gas Chromatography – Mass Spectrometry (GC-MS). Even though the Manoyl Oxide calibration line had been made with standards sent by them, no calibration had been made for the 9-hydroxy-Manoyl Oxide. The lack of standards from this terpenoid with previously known concentrations kept us from doing it.

When the results arrived from Bielefeld, it was noticed that much larger amounts of product had been measured in their detection equipment than in ours. This could provide an explanation to why lower terpenoid titres were obtained in the experiments in the *Algaebator*, when compared to the ones mentioned by Lauersen *et al.* (2018). In fact, if we try to estimate the values based on the few samples submitted from the second *Algaebator* experiment, an average of 20 $mgg^{-1}day^{-1}$ from Manoyl Oxide is obtained, almost twice the one registered by Lauersen *et al.* (2018).

The ratio between the concentration values detected by Bielefeld's GC-MS and our GC-FID was not constant, varying a lot with the sample's origin. For this reason, no general conversion was made, and the originally measured values were used. However the general trend would have remained the same.

5. Conclusion

The B1 and B2 strains have shown similar growth rates and Manoyl Oxides titres, except for the fact that only the B2 strain produces 9-hydroxy-Manoyl Oxide. Even so, the terpenoid mostly produced by this strain is still Manoyl Oxide.

The microalgae showed no light sensitivity up to 636 μE. Even though the culture growing at 1877 μE showed evidences of being under stress, there were other factors contributing for it, and further research should be done in order to determine when does photoinhibition occur.

The productivities obtained for the cultures growing in batch in Erlenmeyer flasks, up to 6.8 mg of Manoyl Oxide and 2.4 mg of 9-hydroxy-Manoyl Oxide per gram of dry biomass per day, were lower than the ones recorded in literature, which could be due to an erroneous quantitative analysis.

It was possible to continuously extract both terpenoids in a circulating system, even though a smaller mass transfer area to volume ratio and a lower contact time between the cells and the extraction solvent led to smaller titres. Something to bear in mind while building such a set-up, is to assure a culture flow fast enough to prevent biomass deposits.

Optimizing the growth conditions, such as biomass concentration, incident light intensity and medium composition, would improve the production rate. For Manoyl Oxide, a higher biomass concentration and primary light increase its production, while a maximum for 9-hydroxy-Manoyl Oxide production seems to have been found for a biomass concentration around 1.4 g/L at 636 μE of light intensity.

This continuous extraction system was developed for Manoyl Oxide and its hydroxylated variant, but it could be easily applied to any other *C. reinhardtii* strain producing any other terpenoid.

6. Recommendations and Perspectives

The analytical methods should be improved, namely the accuracy of the GC-FID calibration. Given that the compounds of interest cannot be acquired in previously known concentrations, a more recent calibration line should be made with a similar terpenoid. Additionally, an internal standard, such as valencene or α-humulene amongst others, should be added both for the calibration and all the experimental samples, so that the lack of reproducibility from the GC-FID does not impact the results.

The protocol for Manoyl Oxide quantification in the culture medium and inside the cells (Annex 3) was adapted from the one developed at Bielefeld University, kindly shared by Thomas Baier. It is a very simple and straight forward extraction protocol and given the low precision of the samples treated according to it, an optimization of the procedure could be valuable for more trustworthy results.

A medium optimization should be undertaken in order to understand which are the most crucial trace elements for the growth of this strain and terpenoid production, to eventually increase their concentration and decrease the least significant ones. If this won't impact much the operational cost at lab scale, it will play a fundamental role in assuring a cost-effective process when scaling it up. After all, TAP Medium recipe is almost 55 years old – perhaps it's time for some changes. Additionally, this is a commonly used recipe for Chlamydomonas, but being a GMO strain who overproduces an uncommon product, its metabolic needs will most likely differ from the wild type. During the course of this thesis, besides removing acetic acid and increasing the amount of nitrogen and phosphorus, a small experiment was made with a different buffer: 3-N-Morpholino propanesulfonic acid (MOPS). There are records from nutrients limitation due to complexation caused by TRIS buffer (Ferreira *et al.* 2015). Looking at the buffers without known complexation issues for the working pH and with adequate solubility (Ferreira *et al.* 2015; Yu *et al.* 1997) MOPS was the best option. Erlenmeyers were inoculated with both TP and MP medium (exactly the same as TP medium but with MOPS as buffer), but as no significant difference was seen between them, TRIS was continued to be used in the main experiments. More effort should be put into this topic, and eventually the buffer should be removed for a larger scale up. The buffer was kept in these particular cases given the slow reduction of the reactor's control input to decrease the base addition. In another words, every time the pH would decrease enough for the base pump to be turned on, the base addition input would be reduced in steps of 5% every 30 seconds, often leading to an excessive increase in pH, which could be even more severe with the buffer present in the medium. This shouldn't be a problem in larger reactors with different control systems, where the buffer would only increase the costs.

To assure the reactors were working at steady state, a turbidostat control was used, which bases himself on the measurements from the secondary light. However, at very low values of outgoing light, significant changes in biomass concentration will translate into only very small variations of this parameter, which hardens keeping the biomass density constant. A solution could be controlling the reactor in chemostat mode instead of turbidostat. When the reactor is operated in chemostat, the medium is pumped at a set flow rate, which must not be higher than the growth rate in order to prevent a wash out (Mooij 2012).

The high affinity from Manoyl Oxide and its functionalized version to dodecane may be beneficial for increasing the extraction's efficiency, but it becomes problematic when we start thinking on the following

steps: how to separate the products from the extraction solvent. Given the boiling points from MO and dodecane are 338 ºC (The Good Scents Company) and 216 ºC (ChemSpider) a flash distillation could be a possibility. However, one should assess the thermal degradation of the compound during such process. A back extraction would work only for 9-hydroxy-Manoyl Oxide and an extremely high working pH would be needed, along with large quantities of solvents. Given that mostly Manoyl Oxide is being produced, this method would be insufficient for the current strain. For the eventual application of this work in the bioenergy field with the GMO strains producing bisabolene, there is one more thing to consider when using dodecane as an extraction solvent. Dodecane is a component from gasoline, being fossil fuels its main origin (ECHA). That being said, we would be using large quantities of a fuel to obtain smaller amounts of a potential bio-diesel fuel, which is, to be fair, pointless. Even when applied to extract the precursors of forskolin, one must have this fact into consideration, as it compromises the sustainability of the process.

Alternative extraction methods should then be considered. By using membranes separating the solvent from the culture, solvents such as ethanol could be used, which would be far easier to separate from the products but are toxic when in direct contact with the cells. Another option would be the use of XAD-4 resins (Lanting 2019), which once again would avoid the direct contact between the culture and the extraction solvent, thus allowing the utilization of more toxic but more efficient ones. One should also think on a way of recycling the solvent once the product has been recovered, in order to reduce both costs and the environmental impact of the process.

The final step would be, of course, a larger scale up and how to integrate the designed system to a tubular photobioreactor. In such reactors, the air needs to frequently pass through an air stripper, in order to remove the oxygen and replace it with carbon dioxide. The XAD-4 resins could be integrated in that system, else in a particular vessel specifically in place for the extraction.

In parallel to the described improvements of the process, there is also still room for strain improvement. As previously mentioned, the genetical modifications were induced in a strain which originally could not up take nitrates, nor had a flagellum. Both these characteristics are disadvantageous for larger production. Even though ammonia is a cheaper nitrogen source than nitrates, the overall operational cost might be higher considering that it demands additional base for pH control (Sigma Aldrich) The reduced mobility of the cells due to their lack of flagella increases their deposition on any surface, which may increase clogging or other similar operational issues, besides hardening the cleaning of all used material. Finally, *C. reinhardtii* is a freshwater microalga, therefore requires potable water for its production and has a bigger risk of contamination than saltwater strains. One of the goals from the MERIT project was also to obtain a GMO strain from *Phaeodactylum tricornutum*, a saltwater strain, which would in one strike solve all the strain-related problems mentioned above. However, given the reduced knowledge about the genome and metabolism of this alga compared to *C. reinhardtii,* it is a far more challenging task.

To conclude, there is still a long way to go until large-scale terpenoid production from microalgae is technical and economically feasible, but it promises to be a rewarding path.

7. References

Algenol. n.d. “Algenols Direct to Ethanol Technology A Cyanobacteria-Based Photosynthetic Process for the Production of Ethanol.” Retrieved September 28, 2019 (https://pt.slideshare.net/FrankJochem/algenolsdirecttoethanoltechnologyacyanobacteriabasedphotosyntheticprocessfortheproductionofethanolv2).

Applikon. n.d. “Applikon.” Retrieved October 1, 2019 (https://www.applikon-biotechnology.com).

Bahadar, Ali and M. Bilal Khan. 2013. “Progress in Energy from Microalgae: A Review.” *Renewable and Sustainable Energy Reviews* 27(July 2013):128–48.

Benvenuti, G. 2016. “Batch and Repeated-Batch Oil Production by Microalgae.” Wageningen University & Research.

Biofuels Digest. n.d. “Biofuels Digest.” Retrieved October 13, 2019 (https://www.biofuelsdigest.com/bdigest/2016/05/31/cathay-sets-biofuels-based-flight-record-as-new-a350-ushers-in-renewable-jet-era-at-hong-kong/).

Boeck, Renée De. 2019. “Designing an In-Situ Extraction of Manoyl Oxide Produced by Chlamydomonas Reinhardtii.” Wageningen University & Research.

Borowitzka, Michael A. 2016. “The Physiology of Microalgae.” *The Physiology of Microalgae* 655–81.

Boyle, Nanette R. and John A. Morgan. 2009. “Flux Balance Analysis of Primary Metabolism in Chlamydomonas Reinhardtii.” *BMC Systems Biology* 3:1–14.

Breuer, Guido, Packo P. Lamers, Dirk E. Martens, René B. Draaisma, and René H. Wijffels. 2013. “Effect of Light Intensity, PH, and Temperature on Triacylglycerol (TAG) Accumulation Induced by Nitrogen Starvation in Scenedesmus Obliquus.” *Bioresource Technology* 143:1–9.

Chemicalize. n.d. “Chemicalize.” Retrieved October 11, 2019 (https://chemicalize.com).

ChemSpider. n.d. “Dodecane.” Retrieved October 30, 2019 (http://www.chemspider.com/Chemical-Structure.7890.html).

Chisti, Yusuf. 2007. “Research Review Paper: Biodiesel from Microalgae.” *Biotechnology Advances* 25:294–306.

Chlamydomonas Resource Center. n.d. “Chlamydomonas Resource Center.” Retrieved October 4, 2019 (https://www.chlamycollection.org/product/cc-4350-cw15-nit1-nit2-arg7-8-mt-matagne-302/).

Coleus. n.d. “Coleus.” Retrieved March 6, 2019 (https://www.webmd.com/vitamins/ai/ingredientmono-1044/coleus).

Davies, D. Roy and A. Plaskitt. 1971. “Genetical and Structural Analyses of Cell-Wall Formation in Chlamydomonas Reinhardi.” *Genetical Research* 17(1):33–43.

Davies, Fiona K., Victoria H. Work, Alexander S. Beliaev, and Matthew C. Posewitz. 2014. “Engineering Limonene and Bisabolene Production in Wild Type and a Glycogen-Deficient Mutant of Synechococcus Sp. PCC 7002.” *Frontiers in Bioengineering and Biotechnology* 2(JUN):1–11.

Dictionary of natural Products. n.d. “Dictionary of Natural Products.” Retrieved March 6, 2019 (http://dnp.chemnetbase.com).

Dunstan, G. A., J. K. Volkman, S. M. Barrett, and C. D. Garland. 1993. “Changes in the Lipid Composition and Maximisation of the Polyunsaturated Fatty Acid Content of Three Microalgae Grown in Mass Culture.” *Journal of Applied Phycology* 5(1):71–83.

ECHA. n.d. “Dodecane.” Retrieved October 30, 2019 (https://echa.europa.eu/registration-dossier/-/registered-dossier/13433).

Esquível, Maria G., Helena M. Amaro, Teresa S. Pinto, Pedro S. Fevereiro, and F. Xavier Malcata. 2011. “Efficient H2 Production via Chlamydomonas Reinhardtii.” *Trends in Biotechnology* 29(12):595–600.

Farnesene net. n.d. “Farnesene Net.” Retrieved October 13, 2019 (http://farnesene.net).

Ferreira, Carlos M. H., Isabel S. S. Pinto, Eduardo V. Soares, and Helena M. V. M. Soares. 2015. “(Un)Suitability of the Use of PH Buffers in Biological, Biochemical and Environmental Studies and Their Interaction with Metal Ions-a Review.” *RSC Advances* 5(39):30989–3.

Gallaher, Sean D., Sorel T. Fitz-Gibbon, Anne G. Glaesener, Matteo Pellegrini, and Sabeeha S. Merchanta. 2015. “Chlamydomonas Genome Resource for Laboratory Strains Reveals a Mosaic of Sequence Variation, Identifies True Strain Histories, and Enables Strain-Specific Studies.” *Plant Cell* 27(9):2335–52.

Gorman, D. S. and R. P. Levine. 1965. “Cytochrome f and Plastocyanin: Their Sequence in the Photosynthetic Electron Transport Chain of Chlamydomonas Reinhardi.” *Proceedings of the National Academy of Sciences of the United States of America* 54(6):1665–69.

Griffiths, Melinda J., Clive Garcin, Robert P. van Hille, and Susan T. L. Harrison. 2011. “Interference by Pigment in the Estimation of Microalgal Biomass Concentration by Optical Density.” *Journal of Microbiological Methods* 85(2):119–23.

Guedes, Ana Catarina, Helena M. Amaro, and Francisco Xavier Malcata. 2011. “Microalgae as Sources of Carotenoids.” *Marine Drugs* 9(4):625–44.

Guo, Xiaoyan, Jingjing Liu, Chuanbo Zhang, Fanglong Zhao, and Wenyu Lu. 2019. “Stepwise Increase in the Production of 13R-Manoyl Oxide through Metabolic Engineering of Saccharomyces Cerevisiae.” *Biochemical Engineering Journal* 144(August 2018):73–80.

Gupta, P. and S. C. Phulara. 2015. “Metabolic Engineering for Isoprenoid-Based Biofuel Production.” *Journal of Applied Microbiology* 119(3):605–19.

Halim, Ronald, Michael K. Danquah, and Paul A. Webley. 2012. “Extraction of Oil from Microalgae for Biodiesel Production: A Review.” *Biotechnology Advances* 30(3):709–32.

Harris, Elizabeth H. 1989. “Chlamydomonas in the Laboratory.” *The Chlamydomonas Sourcebook* 241–302.

Healthline. n.d. “Healthline.” Retrieved March 6, 2019 (https://www.healthline.com/nutrition/forskolin-review#section6).

Holmborn, Jonas. 2015. *Alternative Fuels for Internal Combustion Engines - A Literature Review on Fuel Properties to Guide Future Fuel Candidates for Internal Combustion Engines*.

Hyams, Jerry and D. Roy Davies. 1972. “The Induction and Characterisation of Cell Wall Mutants of Chlamydomonas Reinhardi.” *Mutation Research - Fundamental and Molecular Mechanisms of Mutagenesis* 14(4):381–89.

Ignea, Codruta, Efstathia Ioannou, Panagiota Georgantea, Fotini A. Trikka, Anastasia Athanasakoglou, Sofia Loupassaki, Vassilios Roussis, Antonios M. Makris, and Sotirios C. Kampranis. 2016. “Production of the Forskolin Precursor 11β-Hydroxy-Manoyl Oxide in Yeast Using Surrogate Enzymatic Activities.” *Microbial Cell Factories* 15(1):1–11.

Islam, Muhammad Aminul, Kirsten Heimann, and Richard J. Brown. 2017. “Microalgae Biodiesel: Current Status and Future Needs for Engine Performance and Emissions.” *Renewable and Sustainable Energy Reviews* 79(May):1160–70.

Joint BioEnergy Institute. n.d. “Alternative Diesel Fuel from Biosynthetic Bisabolene EIB-2837.” Retrieved April 29, 2019 (https://ipo.lbl.gov/lbnl2837/).

Khan, Muhammad Imran, Jin Hyuk Shin, and Jong Deog Kim. 2018. “The Promising Future of Microalgae: Current Status, Challenges, and Optimization of a Sustainable and Renewable Industry for Biofuels, Feed, and Other Products.” *Microbial Cell Factories* 17(1):1–21.

Khatun, Selima. 2011. “The Strategies for Production of Forskolin Vis-a-Vis Protection Against Soil Borne Diseases of the Potential Herb Coleus Forskohlii Briq.” *European Journal of Medicinal Plants* 1(1):1–9.

Kleinegris, D. 2010. *Milking of Microalgae Revisited*. Vol. 22.

Klok, A. J., P. P. Lamers, D. E. Martens, R. B. Draaisma, and R. H. Wijffels. 2014. “Edible Oils from Microalgae: Insights in TAG Accumulation.” *Trends in Biotechnology* 32(10):521–28.

Klok, Anne. 2013. *Optimization of Lipid Production in Microalgae*.

Kumar, Gopalakrishnan, Sutha Shobana, Wei Hsin Chen, Quang Vu Bach, Sang Hyoun Kim, A. E. Atabani, and Jo Shu Chang. 2017. “A Review of Thermochemical Conversion of Microalgal Biomass for Biofuels: Chemistry and Processes.” *Green Chemistry* 19(1):44–67.

Laane, C., R. Hilhorst, and C. Veeger. 1987. “Design of Reversed Micellar Media for the Enzymatic Synthesis of Apolar Compounds.” *Methods in Enzymology* 136(1984):216–29.

Lanting, Marc. 2019. “In-Situ Extraction and Back-Extraction of Manoyl Oxide Produced by Chlamydomonas Reinhardtii.” Wageningen University & Research.

Lauersen, Kyle J., Julian Wichmann, Thomas Baier, Sotirios C. Kampranis, Irini Pateraki, Birger Lindberg Møller, and Olaf Kruse. 2018. “Phototrophic Production of Heterologous Diterpenoids and a Hydroxy-Functionalized Derivative from Chlamydomonas Reinhardtii.” *Metabolic Engineering* 49(July):116–27.

Laurens, Lieve M. L. 2017. *State of Technology Review – Algae Bioenergy*.

Legere, Ed, Paul Roessler, Harlan Miller, Laura Belicka, Yanhui Yuan, Ron Chance, Kofi Dalrymple, William Porubsky, John Coleman, Kevin Sweeney, Pat Ahlm, and Quang Ha. 2017. “Integrated Pilot-Scale Biorefinery for Producing Ethanol from Hybrid Algae.”

LGem. n.d. “LGem.” Retrieved October 1, 2019 (https://lgem.nl).

Luo, Dexin, Zushou Hu, Dong Gu Choi, Valerie M. Thomas, Matthew J. Realff, and Ronald R. Chance. 2010. “Life Cycle Energy and Greenhouse Gas Emissions for an Ethanol Production Process Based on Blue-Green Algae.” *Environmental Science and Technology* 44(22):8670–77.

MERIT. n.d. “MERIT Project.” Retrieved October 27, 2019 (http://merit-project.net/project.php).

Molazadeh, Marziyeh, Hossein Ahmadzadeh, Hamid R. Pourianfar, Stephen Lyon, and Pabulo

Henrique Rampelotto. 2019. “The Use of Microalgae for Coupling Wastewater Treatment with CO 2 Biofixation.” *Frontiers in Bioengineering and Biotechnology* 7(MAR).

Mooij, Tim De. 2012. “Algaemist Manual.” (November 2011).

Neupert, Juliane, Daniel Karcher, and Ralph Bock. 2009. “Generation of Chlamydomonas Strains That Efficiently Express Nuclear Transgenes.” *Plant Journal* 57(6):1140–50.

Nielsen, Morten T., Johan Andersen Ranberg, Ulla Christensen, Hanne Bjerre Christensen, Scott J. Harrison, Carl Erik Olsen, Björn Hamberger, Birger Lindberg Møller, and Morten H. H. Nørholm. 2014. “Microbial Synthesis of the Forskolin Precursor Manoyl Oxide in an Enantiomerically Pure Form.” *Applied and Environmental Microbiology* 80(23):7258–65.

Pateraki, Irini, Johan Andersen-Ranberg, Niels Bjerg Jensen, Sileshi Gizachew Wubshet, Allison Maree Heskes, Victor Forman, Björn Hallström, Britta Hamberger, Mohammed Saddik Motawia, Carl Erik Olsen, Dan Staerk, Jørgen Hansen, Birger Lindberg Møller, and Björn Hamberger. 2017. “Total Biosynthesis of the Cyclic AMP Booster Forskolin from Coleus Forskohlii.” *ELife* 6:1–28.

Peralta-Yahya, Pamela P., Mario Ouellet, Rossana Chan, Aindrila Mukhopadhyay, Jay D. Keasling, and Taek Soon Lee. 2011. “Identification and Microbial Production of a Terpene-Based Advanced Biofuel.” *Nature Communications* 2(1):483–88.

Phytobloom. n.d. “Phytobloom by Necton.” Retrieved July 24, 2018 (http://phytobloom.com).

Płaczek, Małgorzata, Agnieszka Patyna, and Stanisław Witczak. 2017. “Technical Evaluation of Photobioreactors for Microalgae Cultivation.” *E3S Web of Conferences* 19:1–10.

Roy, Sudeshna Sen and Ruma Pal. 2015. “Microalgae in Aquaculture: A Review with Special References to Nutritional Value and Fish Dietetics.” *Proceedings of the Zoological Society* 68(1):1–8.

Sigma Aldrich. n.d. “Amberlite® XAD4.” Retrieved October 22, 2019a (https://www.sigmaaldrich.com/catalog/product/sigma/xad4?lang=pt&region=PT).

Sigma Aldrich. n.d. “Ammonium Chloride.” Retrieved October 30, 2019b (https://www.sigmaaldrich.com/catalog/search?term=12125-02-9&interface=CAS No.&N=0&mode=partialmaxfocus=product&lang=pt&region=PT&focus=product&gclid=EAIaIQobChMI-8XZ3LrF5QIVFZ3VCh1B5gyBEAAYASAAEgKBlvD_BwE).

Sigma Aldrich. n.d. “Sodium Hidroxide.” Retrieved October 30, 2019c (https://www.sigmaaldrich.com/programs/research-essentials-products.html?TablePage=102880906).

Sigma Aldrich. n.d. “Sodium Nitrate.” Retrieved October 30, 2019d (https://www.sigmaaldrich.com/catalog/search?term=NaNO3&interface=All&N=0&mode=partialmax&lang=pt&region=PT&focus=product).

Strobel, Gary Allan. 2015. “Bioprospecting—Fuels from Fungi.” *Biotechnology Letters* 37(5):973–82.

The Good Scents company. n.d. “The Good Scents Company.” Retrieved October 20, 2019 (http://www.thegoodscentscompany.com/data/rw1019332.html).

The Good Scents Company. n.d. “Manoyl Oxide.” Retrieved October 30, 2019 (http://www.thegoodscentscompany.com/data/rw1539201.html).

De Vree, Jeroen H., Rouke Bosma, Marcel Janssen, Maria J. Barbosa, and René H. Wijffels. 2015. “Comparison of Four Outdoor Pilot-Scale Photobioreactors.” *Biotechnology for Biofuels* 8(1):1–12.

Wei Liu, Xin Xu, Rubing Zhang, Tao Cheng, Yujin Cao, Xiaoxiao Li, Jiantao Guo, Huizhou Liu &. Mo Xian. 2016. “Engineering Escherichia Coli for High-Yield Geraniol Production with Biotransformation of Geranyl Acetate to Geraniol under Fed-Batch Culture.” *Biotechnology for Biofuels* 9(58).

Woods, R. Paul, Edward Legere, Benjamin Moll, and Edwin Malkiel. 2012. “United States Patent: Closed Photobioreactor System for Continued Daily in Situ Production of Ethanol from Geneticall Enhanced Photosynthetic Organisms with Means for Separation and Removal of Ethanol.” 2(12).

Yu, Qiuyue, Ashoka Kandegedara, Yanping Xu, and D. B. Rorabacher. 1997. “Avoiding Interferences from Good’s Buffers: A Contiguous Series of Noncomplexing Tertiary Amine Buffers Covering the Entire Range of PH 3-11.” *Analytical Biochemistry* 253(1):50–56.

Zhuang, Xun, Oliver Kilian, Eric Monroe, Masakazu Ito, Mary Bao Tran-Gymfi, Fang Liu, Ryan W. Davis, Mona Mirsiaghi, Eric Sundstrom, Todd Pray, Jeffrey M. Skerker, Anthe George, and John M. Gladden. 2019. “Monoterpene Production by the Carotenogenic Yeast Rhodosporidium Toruloides.” *Microbial Cell Factories* 18(1):1–15.

Annex 1 – Medium

TAP Medium (1L)	
TRIS (buffer)	2,42 g
TAP Salts Solution	25 mL
p-Solution	375 µL
Hutner's trace Solutions	1 mL each
Acetic Acid 100 %	1 mL

TAP Salts Solution (1L)	
NH_4Cl	16 g
$MgSO_4 \cdot 7\ H_2O$	4 g
$CaCl_2 \cdot 2\ H_2O$	2 g

p- Solution (100 mL)	
KH_2PO_4	14,8 g
K_2HPO_4	28,8 g

Stock Solutions	
1	125 mM EDTA-Na_2 13,959 g EDTA-Na_2 in 300 mL demi-water
2	285 µM $(NH_4)_6Mo_7O_{24}$ 0,088 g $(NH_4)_6Mo_7O_{24}$ in 250 mL demi-water
3	1mM Na_2SeO_3 0,043 g Na_2SeO_3 in 250 mL demi-water

Hutner's trace Solutions	
1. EDTA-Na_2	20 mL Stock Solution 1 Fill to 100 mL demi-water
2. $(NH_4)_6MO_7O_{24}$	10 mL Stock Solution 2 Fill to 100 mL demi-water
3. Na_2SeO_3	10 mL Stock Solution 3 Fill to 100 mL demi-water
4. Zn · EDTA	0,072 g $ZnSO_4 \cdot 7\ H_2O$ 2,2 mL Stock Solution 1 Fill to 100 mL demi-water
5. Mn · EDTA	0,1188 g $MnCl_2 \cdot 4\ H_2O$ 4,8 mL Stock Solution 1 Fill to 100 mL demi-water
6. Fe · EDTA	0,82 g EDTA-Na_2 0,232 g Na_2CO_3 0,54 g $FeCl_3 \cdot 6\ H_2O$ Fill to 100 mL demi-water
7. Cu· EDTA	0,034 g $CuCl_2$ 1,6 mL Stock Solution Fill to 100 mL demi-water

For **Agar plates**, add 15 g/L agar to the medium, autoclave, and then add the following antibiotics: 15 mg/L Paromomycin, 20 mg/L Hygromycin, 200 mg/L Spectinomycin and 10 mg/L Zeocin.

For **TP Medium**, use 10 mL HCl 1M instead of the Acetic Acid 100%.

For **T2P 2N Medium** use a TAP Salts Solution with twice the amount of NH_4Cl and add twice the amount of p-Solution.

Annex 2 – Optical Density and Dry weight calibration

The optical density at a wavelength of 750 nm and dry weight were measured from a set of B2 1mL samples from different origins. Biomass concentration was then calculated and a calibration line between it and the optical density for the B2 strain was built.

Table 5: Samples' Optical Density at 750nm and its biomass concentration used for establishing the correlation between them.

Sample	OD (750 nm)	biomass concentration (mg dry weight/mL)
1	0.536	0.29
2	0.885	0.46
3	1.285	0.68
4	2.120	0.94
5	2.330	1.05
6	4.800	2.19

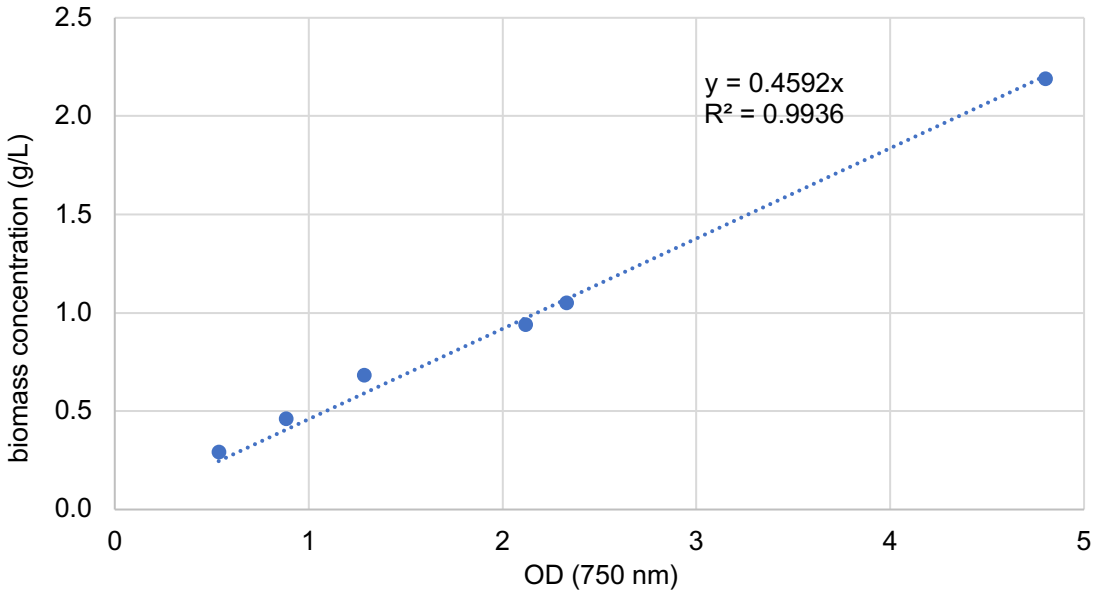

Figure 33: Correlation between the biomass concentration in g dry weight/L of culture and its Optical Density at 750 nm.

Annex 3 – Manoyl Oxide quantification in the culture

The procedure to determine the Manoyl Oxide content in the culture medium and inside the cell was as follows:

1. A 2 mL sample was taken
2. The sample was centrifuged at 875 x g for 10 minutes
3. Place 900 µL of the supernatant with 100 µL of dodecane in an Eppendorf
4. Resuspend the pellet in 2 mL of demi-water
5. Place 900 µL of the resuspended pellet with 100 µL of dodecane in an Eppendorf
6. Place 900 µL of the resuspended pellet in a bead beater
7. Place the content of the bead beater with 100 µL of dodecane in an Eppendorf
8. Place all samples in a spinner for at least 1h
9. Centrifuge all samples at 2500 x g for 10 minutes
10. Take 50 µL from the dodecane layer into a GC-FID veil and analyse it

This same procedure is also represented in the following scheme:

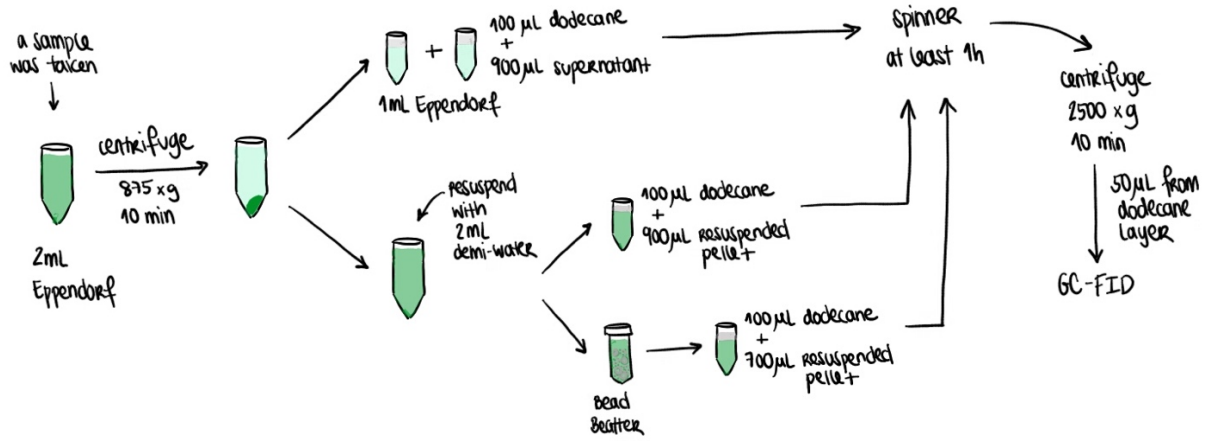

Figure 34: Manoyl Oxide quantification inside the cells and medium procedure scheme.

Annex 4 – Cell viability

The procedure to assess the culture's viable cells percentage was as follows:

1. Dilute the sample if needed, so that the samples have a cell concentration between 500 000 and 1 000 000 cells per mL, which corresponds to an optical density around 4
2. Prepare a stock solution of 4mg Erythrosin B per mL Phosphate Buffered Saline (PBS) solution
3. Add 15 µL stock solution to 100 µL culture
4. Let it incubate for at least 10 minutes
5. Examine it under a microscope in a Neubauer chamber and count the number of viable and non-viable cells

Table 6: Phosphate Buffered Saline (PBS) solution composition.

PBS (1L)	
NaCl	8 g
KCl	200 mg
Na_2HPO_4	1,44 g
KH_2PO_4	240 mg

Annex 5 – GC-FID Method

The temperature programme employed for the analyses was as follows:

1. Initial temperature is 80 ºC
2. Rises to 120 ºC at a rate of 22,042 ºC/min
3. Rises to 160 ºC at a rate of 6,6127 ºC/min
4. Rises to 270 ºC at a rate of 22,042 ºC/min
5. Is held at 270 ºC for one minute
6. Rises to 320 ºC at a rate of 22,042 ºC/min
7. Is held at 320 ºC for 5 minutes to assure all present substances are evaporated

Manoyl Oxide samples with known concentration were provided by the University of Bielefeld. By analysing them in the GC-FID, a calibration line was built, which was then used to calculate the concentrations in all samples.

Table 7: GC-FID readings for Manoyl Oxide known concentrations used to calibrate the GC-FID analysis.

[MO] (ppm)	Area
1	9,599018
5	34,34466
10	37,80686
25	80,69793
100	336,276
150	586,6798

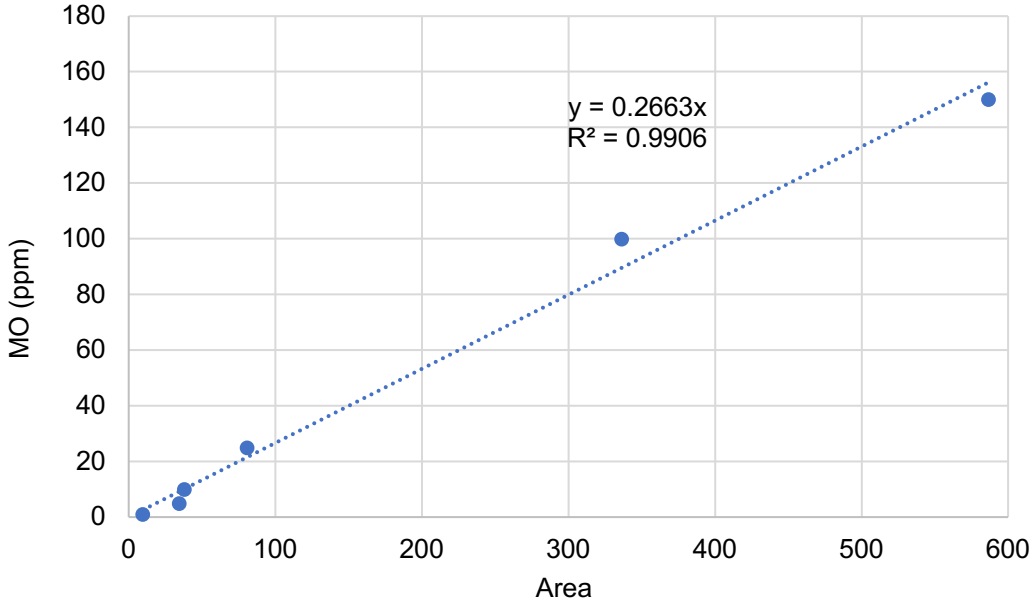

Figure 35: Calibration line for determination of Manoyl Oxide concentration by GC-FID.